NEODYMIUM ISOTOPIC STUDY OF OCEAN CIRCULATION DURING THE MIDDLE TO LATE MIOCENE CARBONATE CRASH

By

DERRICK RICHARD NEWKIRK

A THESIS PRESENTED TO THE GRADUATE SCHOOL
OF THE UNIVERSITY OF FLORIDA IN PARTIAL FULFILLMENT
OF THE REQUIREMENTS FOR THE DEGREE OF
MASTER OF SCIENCE

UNIVERSITY OF FLORIDA

2007

© 2007 Derrick Richard Newkirk

To my grandmother Addie Hair.

ACKNOWLEDGMENTS

I would like to sincerely thank Dr. Ellen Martin for her continued guidance on this project. Not only is she a great mentor, but also a good friend and a pleasure to work with. Thanks also go to my committee members Dr. David Hodell and Dr. John Jaeger for their advice and review of this thesis. Thanks also to Dr. Philip Neuhoff for the many insightful conversations we had pertaining to this research.

I am also very grateful for the financial support that was provided by the NSF SGR grant awarded to Dr. Ellen Martin, the Department of Geological Sciences, and Graduate Student Council.

Special thanks go to Susanna Blair for her guidance and continuous help in the lab at the beginning of my graduate career. Also, I would like to thank Dr. George Kamenov for his assistance in the lab, help with analysis, and suggestions for streamlining laboratory procedures. I would also like to thank Wendell Phillips, Tracy King, Nicole Andersen and the many others who have helped me in the laboratory.

Finally, I would like to thank my family and friends. Thanks go to Pat and Rick Newkirk for their unfaltering love and support. Thanks go to Ryan Newkirk for being a great friend and a very supportive brother. Thanks go to Scottie Andre for playing a huge role in my upbringing and being a good role model. Thanks go to Laura Ruhl for her never ending love, encouragement, and support throughout this process. Thanks go to my many wonderful friends in the Department of Geological Science at UF, especially Jonathan Hoffman, PJ Moore, Branden Kramer, Kris Crocket, Mike Ritorto, Gillian Rosen, and Dorsey Wanless. Thanks to Dr. Gabriel Filippelli for his guidance, friendship, and encouragement to continue on to graduate school. Thanks to Dr. Jennifer Latimer for her guidance, friendship, and invaluable lab guidance that she gave me as an undergraduate researcher. And last but not least thanks go to all of my

wonderful friends outside of the department and from my hometown, especially Jason Wright, Adam Faust, Judd Sparks, Dr. Gifford Waters, Erica Roberts, Carlos Zambrano, and Ryan Fleming.

TABLE OF CONTENTS

LIST OF TABLES

LIST OF FIGURES

Abstract of Thesis Presented to the Graduate School
of the University of Florida in Partial Fulfillment of the
Requirements for the Degree of Master of Science

NEODYMIUM ISOTOPIC STUDY OF OCEAN CIRCULATION DURING THE MIDDLE TO LATE MIOCENE CARBONATE CRASH

By

Derrick Richard Newkirk

August 2007

Chair: Michael R. Perfit
Major: Geology

The term "carbonate crash" describes an extensive dissolution event (or series of events) marked by low carbonate mass accumulation rates (MARs), which were originally observed in middle/upper Miocene sediments from the eastern equatorial Pacific and later discovered in western equatorial Atlantic and Caribbean Basin sediments. The timing of the crash suggests a change in global circulation patterns associated with the shoaling of the Central American Seaway (CAS) may have brought more corrosive bottom waters to this region. This study presents the first neodymium (Nd) isotopic data from this region which has been used to identify the source of bottom waters and the basic circulation patterns in the Caribbean during this gateway event.

The total range for ε_{Nd} values measured for fossil fish teeth over the interval of interest for site 998 (Yucatan Basin) is -6.6 to 0 from 14.1 to 9.0 Ma. Values for site 999 (Colombian Basin) range from -6.4 to -0.1 for 14.0 Ma to 9.1 Ma, and values for site 846 (Peru Basin) range from -3.75 to -1.65 for 14.1 Ma to 8.1 Ma. During the carbonate crash intervals (low carbonate MARs), the ε_{Nd} values shift to more radiogenic values at all three sites. The radiogenic ε_{Nd} values recorded in the Caribbean are similar to Pacific intermediate waters, which suggest the flow of Pacific water from west to east through the CAS into the Caribbean Basin. This flow pattern

agrees with several general ocean circulation models studying the shoaling of the Isthmus of Panama, as well as $\delta^{13}C$ data.

Middle to late Miocene Caribbean carbonate crash episodes also appear to correlate to intervals of increased production of Northern Component Water (NCW). For the Caribbean, periods of enhanced conveyor circulation associated with enhanced NCW production appear to correlate with intervals when older, more corrosive intermediate Pacific waters passed through the CAS. Increased carbonate preservation in the Caribbean following the carbonate crash coincides with decreasing NCW production and less radiogenic ε_{Nd} values, suggesting a gradual decline in Pacific waters flowing into the Caribbean Basin as the Isthmus of Panama shoaled.

In the Pacific, increased NCW production resulted in a greater contribution of NCW to Circumpolar Water (CPW) and therefore older, more corrosive CPW, which ultimately formed more corrosive North Pacific Intermediate Water (NPIW) and Pacific Central Water (PCW). The southward migration of these water masses is documented by the progression of low carbonate MARs starting in the northern section of the eastern equatorial Pacific near the CAS at ~12 Ma, and moving further south to the location of site 846 by ~11.5 Ma. The carbonate crash interval at site 846 correlates with ε_{Nd} values that shift upward to ~-2, a value consistent with the introduction of corrosive NPIW to this site.

CHAPTER 1
INTRODUCTION

The term "carbonate crash" was coined by Lyle et al. (1995) to describe an extensive dissolution event (or series of events), marked by low carbonate mass accumulation rates (MAR) during the middle/late Miocene that were observed during Ocean Drilling Program (ODP) Leg 138 in the eastern equatorial Pacific (Farrell et al., 1995; Lyle et al., 1995). Subsequently, carbonate crash events have also been documented in the western equatorial Atlantic (Leg 154; King et al., 1997; Shackleton and Crowhurst, 1997), and the Caribbean (Leg 165; Roth et al., 2000) (Figure 1-1). Theories for the carbonate crash include: 1) increased productivity resulting in enhanced decay (oxidation) of organic matter on the seafloor, or 2) a change in global thermohaline circulation that introduced more corrosive bottom water to the equatorial region.

Lyle et al. (1995) noted that increased surface productivity and the associated production of acid in the deep ocean during the degradation of large quantities of organic carbon would lead to more corrosive bottom waters, resulting in a decrease in carbonate MAR. However, Lyle et al. (1995) argued against this mechanism based on a lack of evidence for increased C_{org} MAR at the time of the carbonate crash in the eastern equatorial Pacific, as well as a lack of a covariance between carbonate and opal MARs. Specifically, Lyle et al. (1995) believed increased surface productivity and associated deep water acidity should result in an increased C_{org} MAR and opal MAR, and decreased carbonate MAR.

Alternatively, the carbonate crash may have resulted from a change in deep ocean circulation. In this scenario, intervals of low carbonate MAR are linked to the presence of more corrosive intermediate and deep water masses at sites around the Caribbean region that supply deep waters to the Caribbean Basin (Roth et al., 2000; Lyle et al., 1995; Farrell et al., 1995). The

timing of the crash also suggests changing circulation patterns may have been associated with the shoaling of the Central American Seaway (CAS).

Openings and closings of oceanic gateways have been associated with reorganizations of ocean circulation and have been linked to dramatic climatic events throughout geologic time. An example of this is the opening of the Tasman Seaway and the Drake Passage, which have been linked to the onset of the Antarctic Circumpolar Current (ACC), the thermal isolation of Antarctica, and the development of ice sheets on Antarctica (Kennett et al., 1974; Kennett, 1977; Exon et al., 2002; Scher and Martin, 2006).

Previous studies of the effect of the closure of the CAS have focused on large- scale changes in surface ocean circulation and the resulting impact on climate (Keigwin, 1982; Keller et al., 1989; Coates et al., 1992; Moore et al., 1993; Haug and Tiedemann, 1998). However, this closure likely impacted deep water circulation patterns as well. Closure presumably redirected warm, saline surface waters from the Gulf of Mexico to the North Atlantic, thereby increasing the salinity and density of the deep water formed in the Norwegian-Greenland-Labrador Seas. This increase in North Atlantic Deep Water (NADW) production would have occurred at the expense of North Atlantic Intermediate Water (NAIW), and the reduced NAIW would have been compensated by northward migration of Antarctic Intermediate Water (AAIW). In this scenario, the water mass flowing over the shallow sills separating the Caribbean from the Atlantic would depend on the position of the boundary between these two intermediate water masses. According to Roth et al. (2000), the water mass that overflowed the shallow to intermediate sills and filled the deep Caribbean during times of enhanced carbonate preservation was primarily sourced from the north, while southern sourced waters dominated during corrosive intervals.

In this scenario, the Southern Ocean becomes the primary location for deep-water formation during times of decreased NADW production. Thus, the deep water in the Pacific travels a shorter distance resulting in a water mass with higher oxygen and lower nutrient levels. A similar process is observed in the eastern equatorial Pacific during glacial stages, which are accompanied by weaker NADW production. Le et al. (1995) observed greater carbonate preservation in the eastern equatorial Pacific during glacial stages and greater dissolution during interglacial. When NADW production is strong, the deep water in the Pacific has to travel from the North Atlantic. This longer travel path allows for more oxidation of organic matter, resulting in increased concentrations of CO_2 and nutrients, while decreased oxygen concentrations, and older, more corrosive bottom water in the eastern equatorial Pacific.

This mechanism for the carbonate crash presented by Roth et al. (2000) is based on a model developed by Haddad and Droxler (1996) to account for Pleistocene deposits in the Caribbean that alternate between low carbonate accumulation during interglacial periods, and carbonate deposition during glacial periods. Haddad and Droxler (1996) suggested that high rates of NADW production during interglacial periods resulted in corrosive AAIW overflowing the Caribbean sill and filling the Caribbean Basin, while decreased NADW production during glacial periods resulted in NAIW overflowing the Caribbean sill and filling the Caribbean Basin. Roth et al. (2000) attempted to use carbon isotopic data to identify the source of water entering the Caribbean Basin and test this theory. They interpreted changes in $\delta^{13}C$ based upon the assumption that either NAIW or AAIW was overflowing the sill to fill the Caribbean Basin, but they could not identify a specific water mass with this proxy. Carbon isotopes can give an indication of the age of the water mass, but they are not a unique proxy for water mass because they are not conservative tracers (Kroopnick, 1985). In addition, carbon isotopic data are

generally recovered from foraminifera, which are rarely preserved during dissolution events (Shackleton and Hall, 1995, 1997; Roth et al., 2000).

The goal of this study is to use neodymium (Nd) isotopes preserved in fossil fish teeth to test theories about ocean circulation during the middle/late Miocene carbonate crash. Neodymium isotopes were used because they are generally viewed as "quasi-conservative" tracers of water masses, meaning they reflect the initial signal of the source region, but can be modified by weathering inputs during circulation (Frank et al., 2003; Goldstein and Hemming, 2003). The end-member Nd isotopic compositions of the water masses in the Miocene are relatively well constrained by published data for Fe-Mn crusts and fish teeth (Burton et al., 1997 and 1999; Ling et al., 1997; O'Nions et al., 1998; Martin and Haley, 2000; Frank et al., 2002; van de Flierdt et al., 2004; Scher and Martin, 2004). In addition, fossil fish teeth are abundant throughout the dissolution events, making them excellent archives to reconstruct paleocirculation during these events.

Results of this research support the hypothesis that changes in deep water circulation are associated with the carbonate crash intervals in the Caribbean and Pacific; however, the most corrosive bottom waters appear to be derived from the Pacific rather than the Atlantic. This scenario suggests west to east flow through the CAS in the middle Miocene in response to the shoaling of the CAS and Northern Component Water (NCW) production.

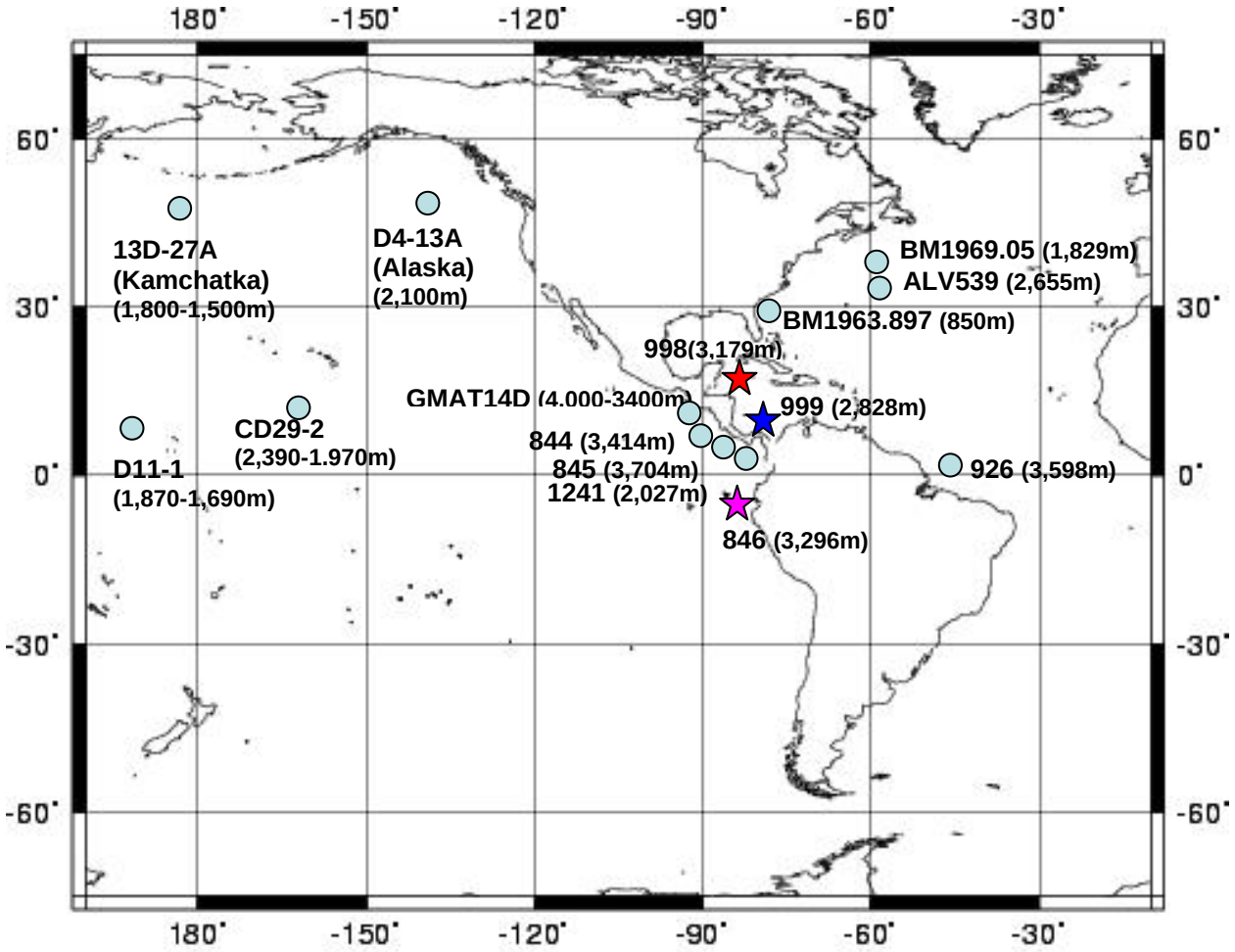

Figure 1-1. Plate reconstruction from the Ocean Drilling Stratigraphic Network (www.odsn.de) with ODP and Ferromanganese Crust Locations discussed in this study.

CHAPTER 2
BACKGROUND

2.1 Neodymium Isotope Systematics

The light REE (Rare Earth Element) Neodymium (Nd) has seven isotopes. ^{143}Nd is the radiogenic daughter product of ^{147}Sm (half-life = ~$1.06x10^{11}$ years), which is produced by alpha decay. ^{144}Nd is used as a reference because it is a stable isotope, thus the number of atoms should not change as long as the system remains closed. The $^{143}Nd/^{144}Nd$ ratio is reported as ε_{Nd} in order to report small but significant variations as whole numbers. ε_{Nd} is calculated using the equation:

$$\varepsilon_{Nd(0)}=[(^{143}Nd/^{144}Nd)_{sample}/(^{143}Nd/^{144}Nd)_{CHUR}-1] \times 10^4$$

where CHUR (Chondritic Uniform Reservoir) equals the bulk earth $^{143}Nd/^{144}Nd$ of ~0.512638 (DePaolo and Wasserburg, 1976).

The primary sources of Nd to seawater are continentally derived dust, volcanic ash, resuspended detrital sediments, and riverine inputs in the form of either dissolved or particulate material (Goldstein and Jacobsen, 1988; Elderfield, 1988; Spivack and Wasserburg, 1988; Bertram and Elderfield, 1993; Greaves et al., 1994; Henry et al., 1994; Jeandel et al., 1995, Albarede et al., 1997; Frank, 2002; Tachikawa et al., 1999 and 2003). Hydrothermal sources of Nd to the ocean are insignificant, because Nd is quantitatively scavenged by oxides near the mid-ocean ridge (Michard, 1983; German et al., 1990). Nd concentrations in seawater are fairly low, ~4pg/g in deep water, because Nd ions are relatively insoluble and extremely particle reactive. In a situation that has been termed the Nd Paradox, Nd concentrations vary along the path of the global conveyor belt, but Nd isotopes behave as conservative tracers (Goldstein and Hemming, 2003; Lacan and Jeandel, 2001; Jeandel et al., 1995, 1998; Tachikawa et al., 1999a, 1999b; Bertram and Elderfield, 1993). Specifically, Nd concentrations are low in surface waters, but

higher in deep waters, and concentrations in the Pacific are higher than the Atlantic (Goldstein and Hemming, 2003); however, Nd isotopes in modern core tops correlate well with salinity, a conservative property in seawater (See review in Goldstein and Hemming, 2003).

Another important characteristic of Nd is that its residence time in seawater is 600-1000 years (Tachikawa et al., 1999; Elderfield and Greaves, 1982; Piepgras and Wasserburg, 1985; Jeandel et al., 1995); which is shorter than the mixing time of the ocean at ~1500 years (Broecker and Peng, 1982). Due to this relatively short residence time, different ocean basins have distinct Nd isotopic ratios (Table 1), which also vary vertically within the water column (Piepgras and Wasserburg, 1987; Bertram and Elderfield, 1993; Jeandel, 1993). Modern NADW has an ε_{Nd} value of ~ -14, which reflects the weathering of Archean age rocks from the North American craton (Piepgras and Wasserburg, 1987). Modern Pacific deep water has an ε_{Nd} of ~ -4, which is the result of young, circum-Pacific volcanogenic sources (Piepgras and Jacobsen, 1988), while modern North Pacific Intermediate Water (NPIW) reflects an even stronger influence from radiogenic volcanic material and has an ε_{Nd} value of ~ -2.5 (Piepgras and Jacobsen, 1988). Finally, Antarctic Bottom Water (AABW) and Antarctic Intermediate Water (AAIW) have ε_{Nd} of ~ -8 (Piepgras and Wasserburg, 1982; Jeandel, 1993), which represents mixing of the Atlantic and Pacific water masses. For comparison, the analytical uncertainty for Nd isotopic measurements for this study is ± 0.35 ε_{Nd} units. Therefore, the values for the various end members are analytically distinct.

2.2 Archives of Nd Isotopes

Sedimentological archives such as ferromanganese (Fe-Mn) crusts and nodules, Fe-Mn oxide coatings, and fossil fish teeth have been used to estimate the ε_{Nd} values of past water masses. Data from Fe-Mn crusts and nodules illustrate that the major ocean basins have distinct isotopic compositions (Albarede and Goldstein, 1992; Abouchami et al., 1997; Burton et al.,

1997; Ling et al., 1997; Frank and O'Nions, 1998; Frank et al., 1999 and 2002; von Blackenburg and Igel, 1999); however, Fe-Mn crusts yield very low resolution records due to their slow growth rates (1-15mm/Myr; Segl et al., 1984; Puteanus and Halback, 1988). In addition, the crusts have a sparse distribution, which inhibits large-scale sampling because they only grow where sedimentation rates are extremely slow or currents sweep away hemipelagic sediment. Finally, age control for Fe-Mn crusts, which are dated using Be, is poor beyond 10 Ma because ^{10}Be has a half-life of 1.5×10^6 years. Overall, the slow growth rate of the Fe-Mn crusts records long-term trends and variations in ocean circulation, but they do not record the more rapid shifts in circulation that are frequently associated with climatic events because their signal is integrated over time.

Fossil fish teeth, on the other hand, can be dated accurately with the surrounding sediment using magnetostratigraphy, biostratigraphy, and chemostratigraphy, thereby allowing the development of higher resolution records. Fossil fish teeth, which are composed of hydroxyflourapatite, have been shown to be effective recorders of bottom water Nd isotopic values (Elderfield and Pagett, 1986; Martin and Haley, 2000; Thomas et al., 2003; Martin and Scher, 2004; Thomas, 2004; Scher and Martin, 2006). The hydroxyapatites of living fish teeth have Nd concentrations in the ppb range (Wright et al., 1984; Shaw and Wasserburg, 1985), while the hydroxyfluorapatite of fossil fish teeth have Nd concentrations of 100 to 1000 ppm (Wright et al., 1984; Shaw and Wasserburg, 1985; Staudigel et al., 1985; Martin et al., 1995). Fossil fish teeth appear to incorporate Nd during the early diagenetic transformation of hydroxyapatite to hydroxyfluorapatite at the sediment-water interface, while the teeth are still in contact with ocean bottom waters (Wright et al., 1984; Shaw and Wasserburg, 1985; Staudigel et al., 1985; Martin et al., 1995; Martin and Haley, 2000; Martin and Scher, 2004). Martin and

Haley (2000) have demonstrated that fossil fish teeth record similar isotopic ratios to Fe-Mn crusts when they are exposed to similar bottom waters. Given evidence that the initial ε_{Nd} values are preserved over time (Martin and Scher, 2004), the Nd signals from fossil fish teeth have been used by Scher and Martin (2004, 2006), Thomas et al. (2003), Via and Thomas (2006), and Thomas and Via (2007) to track paleocirculation.

2.3 Carbonate MAR

Carbonate mass accumulation rates (CO_3 MARs) are determined by the following equation:

MAR x $CaCO_3$wt% x 100 = CO_3 MAR

To calculate the CO_3 MAR, the bulk mass accumulation rate (bulk MAR) and the calcium carbonate weight content ($CaCO_3$wt%) must be known. The bulk MARs were calculated by multiplying dry bulk density (grams of dry sediment per wet volume in cubic centimeters) by a calculated linear sedimentation rate (m/m.y.) (Roth et al., 2000). The $CaCO_3$wt% was determined for each sample using a carbonate bomb (Roth et al., 2000). Mass accumulation rates and carbonate mass accumulation rates for this study were taken from Roth et al. (2000) for the two Caribbean Basin sites (998 and 999), and from Farrell et al. (1995) for eastern equatorial Pacific (site 846).

It is important to use carbonate MAR rather than $CaCO_3$wt% to identify changes in the carbonate system, because $CaCO_3$wt% is influenced by dilution from other fractions such as terrigenous matter, volcanic ash, and/or silica.

2.4 General Ocean Circulation

The modern general ocean circulation model is controlled by the sinking of cold, saline surface waters in the high latitudes. Initially, water in the desert latitudes of the Atlantic becomes warm due to solar radiation and saline due to evaporation. This warm-saline water then

moves north into the Norwegian-Greenland Sea as part of the Gulf Stream. As the water travels into the North Atlantic it cools. When the water finally reaches the Norwegian-Greenland Sea it cools until it becomes dense enough to set up an inverse density gradient, allowing the dense overlying water mass to sink. This sinking water mass mixes with Labrador Sea water and becomes North Atlantic Deep Water (NADW), which travels along the western margin of the Atlantic and ultimately mixes with Antarctic Bottom Water (AABW) in the Antarctic Circumpolar Current (ACC) to form Circumpolar Deep Water (CDW). This mixture eventually flows northward into the Indian Ocean and Pacific Ocean. Along its circulation paths in the Indian and Pacific Oceans CDW mixes upward with intermediate and surface waters. These Intermediate and surface waters then flow south from the north Pacific to the south Pacific as either North Pacific Intermediate Water (NPIW) or Pacific Central Water (PCW). The southward flowing water leaves the Pacific Ocean either through the Indonesian Seaway or the Drake Passage, ultimately flowing back into the Atlantic Ocean. Once these waters enter the Atlantic Ocean, they follow the surface gyre circulation back to the equatorial region, thereby starting the cycle over again. This circular path of water has been termed the "global conveyor" by Broecker and Peng (1982) and takes approximately 1,500 years to complete (Broecker and Peng, 1982).

The global conveyor can be altered by the closing/opening of oceanic gateways or the introduction of fresh water. The CAS began closing during the middle to late Miocene creating a barrier between the equatorial Atlantic and Pacific Oceans (Roth et al., 2000). The resulting change in circulation may have affected the redistribution of heat and nutrients throughout the ocean.

2.5 Caribbean Basin Tectonic Setting

Today the Caribbean Basin is bound by Central America to the west, the Lesser Antilles and Aves Swell to the east, and the Nicaragua Rise and Greater Antilles to the north (Droxler et al., 1998). The Aves Swell has behaved as a remnant arc since ~55 Ma (Bird et al., 1993), and according to Droxler et al. (1998) the topographic highs experienced neritic conditions from ~50 – 15 Ma based on seismic surveys, drilling, and dredging, and then deeper conditions after 15 Ma. The two intermediate depth passageways (Windward Passage (1500 m) and the Anegada-Jungfern Passage (1800m) (Figure 2-1) were the result of accelerated subsidence of the Aves Swell to depths of 600 m to 1200 m during the middle Miocene (Pinet et al., 1985; summarized in Droxler et al., 1998).

The Nicaragua Rise is a series of carbonate banks and barrier reefs that created a prominent barrier to circulation during the Oligocene to middle Miocene in the Caribbean and spanned from Nicaragua and Honduras to Jamaica (Lewis and Draper, 1990; Droxler et al., 1992, 1998; Cunningham, 1998) (Figure 2-1). According to Droxler et al. (1992), foundering of the Nicaragua Rise occurred in the middle Miocene (~15-12 Ma), but could have begun as early as late early Miocene (20-15 Ma). Faulting along the rise led to the opening of the north/south oriented Pedro Channel and the northern part of the Walton Basin (Cunningham, 1998). .

Using benthic foraminiferal assemblages from Atrato Basin located in the NW corner of South America, Duque-Caro (1990) suggested that the Isthmus of Panama shoaled to a depth of ~2000 m by ~15.9 – 15.1 Ma (ages adjusted to Shackleton et al., 1995a) and to a depth of ~1000 m between 12 – 10.2 Ma (ages adjusted to Shackleton et al., 1995a). Shoaling of the Isthmus of Panama to 100 m occurred by 4.6 Ma and final closure of the Central America Seaway occurred by ~3.5 Ma was suggested by Haug and Tiedemann (1998) based on a salinity increase recorded in planktonic foraminifera.

2.6 Modern Caribbean Basin Circulation

The flow of shallow waters into the Caribbean Basin is controlled by both changes in meridional overturning in the North Atlantic and changes in the position of the Intertropical Convergence Zone (ITCZ) (Johns et al., 2002). According to Johns et al. (2002), almost all of the wind driven flow into the Caribbean occurs north of 15ºN (north of Martinique). During the summer a cyclonic circulation cell sets up southeast of the Lesser Antilles blocking the flow of the Guyana Current into the Caribbean (Muller-Karger et al., 1989) while the ITCZ is located at its northernmost position (6-10ºN) (Philander and Pacanowski, 1986).

Intermediate depth sills that extend from Venezuela to the Greater Antilles restrict flow from the Atlantic into the Caribbean. The two most important connections today are the Windward Passage (1500 m) and the Anegada-Jungfern Passage (1800m) (Pinet et al., 1985; Figure 2-1). Because of these sills, bottom water in the Caribbean Basin is sourced by intermediate depth waters from the Atlantic. Today, the water masses flowing into the Caribbean over these sills are upper NADW (uNADW), which originates at depths of ~1400 - ~3500 m and AAIW, which originates at depths of 800-1400 m (Haddad, 1994; Haddad and Droxler, 1996). These two water masses mix together upon entering and fill the lower reaches of the Caribbean basins as a result of turbulent mixing. Roth (1998) showed that water temperatures below the sill depths in the Caribbean are distinct from waters of the same depth in the Atlantic. Specifically, waters within the Caribbean basin are warmer and more homogeneous. These temperatures indicate that the deep waters filling the Caribbean basins have an origin shallower than 1500 m (Roth, 1998).

2.7 Ocean Circulation Models

Flow of Pacific water through an open CAS into the Atlantic was the result of several general ocean circulation models evaluating the effects of shoaling of the Isthmus of Panama,

NADW production, and the location of the ITCZ (e.g., Mikolajewicz and Crowley, 1997; Nisancioglu et al., 2003; Nof and van Gorder, 2003; Prange and Schultz, 2004; Klocker et al., 2005; Schneider and Schmittner, 2006; Steph et al., 2006). Model results of Schneider and Schmittner (2006) showed that when the isthmus shoaled to 2000 m the deep waters flowed from the Atlantic to the Pacific, while the intermediate (>800 m) and surface waters flowed from the Pacific to the Atlantic. The model presented by Nisancioglu et al. (2003) indicated that Pacific intermediate waters began to flow through the CAS once the Isthmus of Panama shoaled to 1000 meters as a result of steric sea level differences between the Pacific and Atlantic. The production of NADW affected the model results of Nof and Van Gorder (2003). Their results showed that the net transport of water through the CAS would be westward without the formation of NADW, while a high rate of NADW production would lead to eastward flow through the CAS. In the model presented by Steph et al. (2006), the majority of the flow through the CAS was again from the Pacific to the Atlantic as a result of steric sea level differences, with the exception of the Ekman-dominated surface layer. This surface layer is affected when the ITCZ is located in its southernmost location and the northeast trade winds profoundly effect steric sea level differences in the gateway region diminishing the effects at the surface (Steph et al., 2006).

2.8 Description of Sample Sites

2.8.1 ODP Site 846B

Site 846B (3°5.696'S, 90°49.078'W; 3296 m water depth) is located within the Peru Basin (Figure 1-1). Coring recovered a continuous record of the early/middle Miocene boundary at this site (Mayer, Pisias, Janecek, et al., 1992). The total depth of penetration of hole 846B was 422.4 mbsf (meters below seafloor), which corresponds to an age of ~16 Ma (Mayer, Pisias, Janecek, et al., 1992). The samples used in this study came from 272.3 to 371.5 mbsf, which corresponds to an age range of 8.1 to 14.1 Ma. From 272.3 to 317 mbsf (8.1 to 10.8 Ma) the

samples are composed of clayey radiolarian diatom ooze interbedded with minor diatom nannofossil ooze (Mayer, Pisias, Janecek, et al., 1992). From 317 to 371.5 mbsf (10.8 to 14.1 Ma) the sediments are composed of nannofossil ooze with minor amounts of biogenic silica (Mayer, Pisias, Janecek, et al., 1992).

From 14.1 to 11.5 Ma the carbonate MARs ranged from 0.66 to 1.43 g/cm^2 per k.y. (Figure 2-2) (Farrell et al., 1995) with an average value of ~0.9 g/cm^2 per k.y. After 11.5 Ma the carbonate MARs decrease to levels ranging in values between 0.73 and 0.04 g/cm^2 per k.y. until 8 My, with the exception of a spike to ~1.24 g/cm^2 per k.y. at 10.7 Ma (Farrell et al., 1995).

2.8.2 ODP Site 998A

Site 998A (19°29.377'N, 82°56.166'W; 3101 m water depth) is located on the northern flank of the Cayman Rise in the Yucatan Basin (Figure 1-1). A continuous Cenozoic section was recovered recording the evolution of Caribbean ocean circulation (Sigurdsson, Leckie, Acton, et al., 1997). The total depth of penetration of hole 998A was 637.6 mbsf (~50 Ma) (Sigurdsson, Leckie, Acton, et al., 1997). The samples used in this study came from 132.5 to 177.7 mbsf, which corresponds to an age range of 9 to 14 Ma. From 132.5 to 161 mbsf (9 to 12.1 Ma) the samples are composed of nannofossil ooze with clay and nannofossil mixed sediments, and from 161 to 177.7 mbsf (12.1 to 14 Ma) they are composed of clayey nannofossil chalk and nannofossil mixed sediment (Sigurdsson, Leckie, Acton, et al., 1997).

The carbonate MARs ranged between 0.54 and 0.86 g/cm^2 per k.y. with an average of ~0.75 g/cm^2 per k.y. (Figure 2-2) (Roth, 1998). From 12 to 10 Ma the values ranged between 0 and 0.7 g/cm^2 per k.y. with lows from 12-11.8, 11.6-11.4, 11-10.8, 10.6-10.5, and 10.2 Ma (Roth, 1998). After 10 Ma, the values return to an average of ~0.75 g/cm^2 per k.y. (Roth, 1998).

2.8.3 ODP Site 999A

Site 999A (12°44.639'N, 78°44.360'W; 2839 m water depth) is located on the Kogi Rise within the Colombian Basin (Figure 1-1; Sigurdsson, Leckie, Acton, et al., 1997). This site was selected in the hopes of recovering a continuous core that recorded the progressive closure of the Central American Seaway (Sigurdsson, Leckie, Acton, et al., 1997). A total of 566.1 m of core was recovered from site 999A (Sigurdsson, Leckie, Acton, et al., 1997), which correlates to an age of ~22.3 Ma (Peters et al., 2000). The samples used in this study came from 243.9 to 351.4 mbsf, which corresponds to 8.8 to 14 Ma. From 243.9 to 346.9 mbsf (8.8 to 13.8 Ma), the samples are composed of indurated clayey nannofossil to clay with nannofossils, and from 346.9 to 351.4 mbsf (13.8 to 14 Ma) they are composed of clayey calcareous chalk with foraminifers (Sigurdsson, Leckie, Acton, et al., 1997).

Carbonate MARs gradually decrease from ~2 g/cm^2 per k.y. to ~1 g/cm^2 per k.y. from 14.2 to ~12.1 Ma with significant decreases to values <0.5 g/cm^2 per k.y. at 13.55, 13.05, and 12.55 Ma (Figure 2-2) (Roth, 1998). The largest decreases in carbonate MARs occurred between 12 and 10 Ma with values ranging between 0 and 1 g/cm^2 per k.y., with lowest accumulations occurring at 12.0-11.8, 11.6-11.4, 11.0-10.8, 10.6-10.5, and 10.2 Ma (Roth, 1998). Carbonate MAR values increased from ~1 to ~1.5 g/cm^2 per k.y. from 10 to 9 Ma (Roth, 1998).

2.8.4 Age Models

The age/depth model used for site 846B (Figure 2-3) is based on nannofossil biostratigraphy of Raffi and Flores (1995) in which they used zonal boundaries defined by Martini (1971) and Bukry (1973). The ages of these zonal boundaries and magnetic reversals (Mayer, Pisias, Janecek, et al., 1992) were recalibrated to ages determined by Shackleton et al. (1995a) using orbital tuning. The age/depth models for sites 998 and 999 were based on the

same zonal boundaries of Raffi and Flores (1995) and the recalibrated ages of Shackleton et al. (1995a) by Kameo and Bralower (2000). Therefore the age models for all three sites were done using the same age/depth models. Shackleton et al. (1995b) determined that the age uncertainty of the nannofossils was ±0.1 Ma.

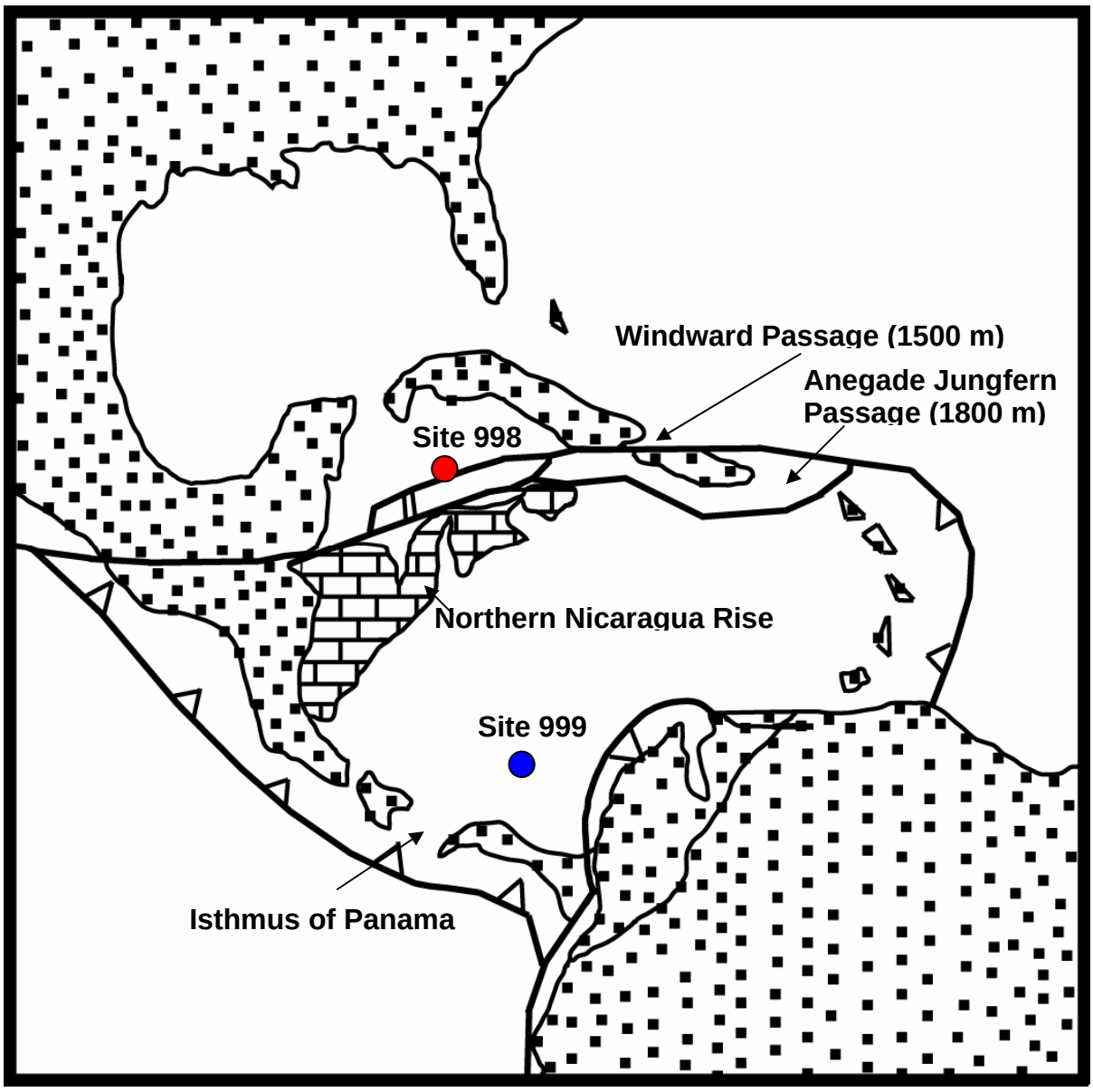

Figure 2-1. Simplified reconstruction of the Caribbean Region illustrating the locations of sites 998 and 999 from this study (after Pindell (1994) and modified from Roth et al. (2000).

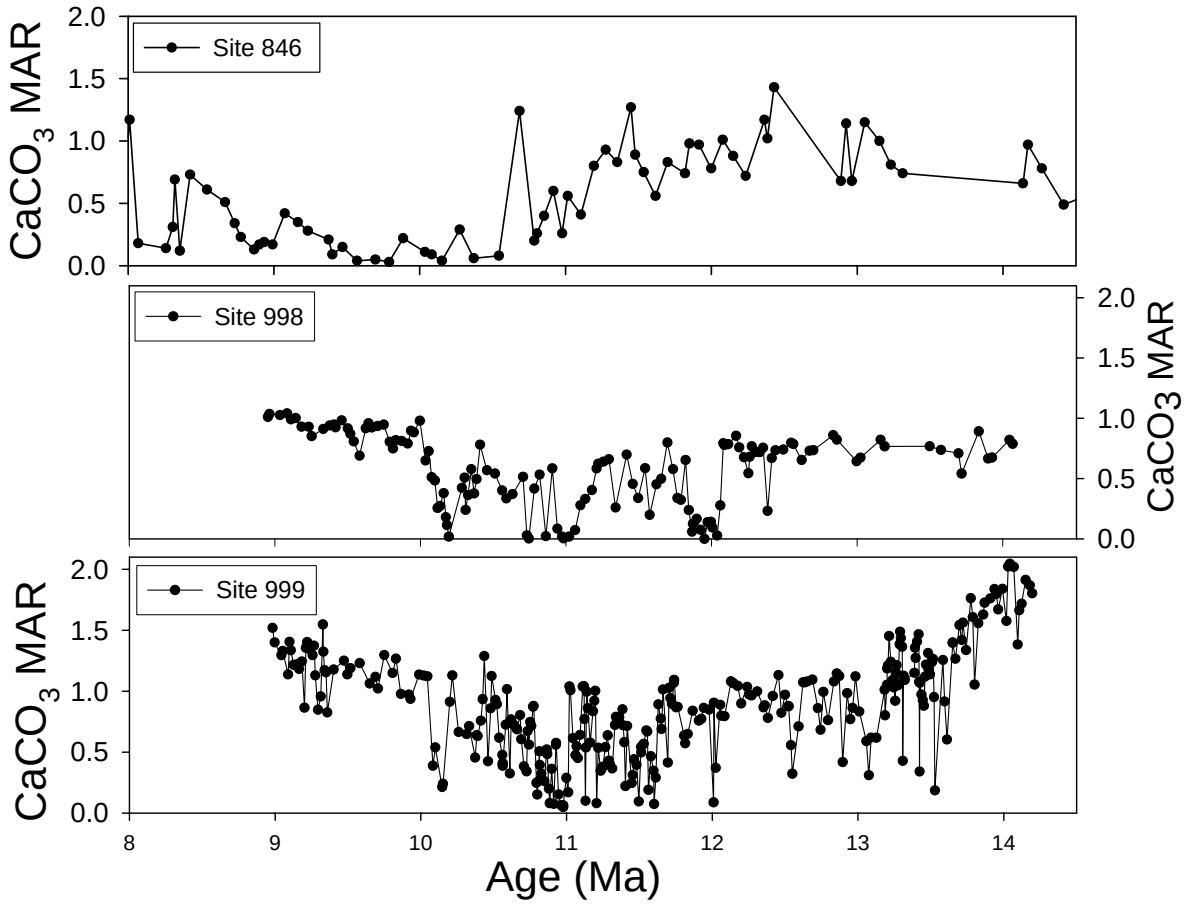

Figure 2-2. Carbonate MAR records for sites 846, 998 and 999 from 8 to 14 Ma from Roth et al. (2000)

CHAPTER 3
METHODS

3.1 Fossil Fish Teeth Sample Preparation

Sediment samples were oven dried, disaggregated and wet sieved prior to picking fossil fish teeth from the >125 μm fraction. The fossil fish teeth were then cleaned using an oxidative/reductive cleaning technique from Boyle (1981) and Boyle and Keigwin (1985). The oxidative/reductive cleaning technique removed organic matter and oxide coatings, which allows for the analysis of isotopic ratios that are purely from the teeth. The cleaned teeth were dissolved in aqua regia to remove additional organic material and then dried prior to the chemical separation of Nd. Concentrations of Nd in the teeth typically range from 100 to 400 ppm (Martin and Haley, 2000), and ~100 μg of cleaned teeth were used for analyses.

3.2 Column Chemistry

Effective isolation of Nd is a two step process. The first set of quartz columns, or primary columns, isolate the bulk rare earth elements (REEs) from the sample using Mitsubishi cation exchange resin with HCl as the eluent. The dissolved teeth were dried and re-dissolved in 50 μL of 0.75 N HCl and the REEs were eluted using 4.5 N HCl after the removal of Ca, Sr, and Ba using a standard procedure (Scher and Martin, 2004). After collection, the bulk REE samples were again dried and re-dissolved with 200 μL of 0.18 N HCl and passed through quartz columns packed with Teflon beads coated with bis-ethylhexyl phosphoric acid, to separate Nd and Sm from the other REE.

3.3 Nd Analysis

Nd isotopic ratios of the fossil fish teeth samples were analyzed using a Nu Plasma Multi-Collector-Inductively Coupled Plasma-Mass Spectrometer (MC-ICP-MS) at the University of Florida. Dried samples were re-dissolved with 0.3 mL of 2% optima HNO_3, then 0.01 mL of the

sample was pipetted into a Teflon sampling beaker and diluted with 0.99 mL of 2% optima HNO_3. Additional acid or sample was added as needed to achieve the ideal voltage range of 2-6 volts for ^{143}Nd. Belshaw et al. (1998) describe the instrument and the optimal operating conditions for the Nu-MC-ICP-MS. JNdi-1 standard was run 5 to 10 times each day, depending on the number of analyses acquired. A daily average for the standard was calculated for each run, and the samples for that run were corrected to the long-term running average of the JNdi-1 standard from the TIMS, which has a $^{143}Nd/^{144}Nd$ of 0.512102 (±0.000012, 2σ). A drift correction was not necessary because variations throughout a run did not indicate a consistent drift. The 2σ error varied on a daily basis, but the long-term 2σ error is 0.35 ε_{Nd} units.

CHAPTER 4
RESULTS

4.1 Neodymium Isotopic Ratios

The total range in ε_{Nd} values at site 846 (Peru Basin) is from -3.75 to -1.65 (Figure 4-1, Table 4-1). In the oldest part of the record at 14.1 Ma, ε_{Nd} begins at -3.75 and slowly shifts to more radiogenic ε_{Nd} values up core (Figure 4-2). From 14.1 to 12.4 Ma the ε_{Nd} values increase to -2.3. From 12.4 to 12.0 Ma ε_{Nd} values shift to less radiogenic values of -3.07. The ε_{Nd} values increase to ~-2.0 at 12.0 Ma and generally remain near that value until 8.4 Ma with a brief shift to -2.93 at 10.6 Ma. After 8.4 Ma ε_{Nd} decreases to -2.9 at 8.1 Ma. The range in ε_{Nd} values at site 846 (Peru Basin) is much smaller than the Caribbean sites.

The total range for ε_{Nd} values over the interval of interest at site 998 (Yucatan Basin) is from -6.6 to 0 (Figure 4-1,Table 4-2). The ε_{Nd} values remain relatively constant ~-4.0 from 14.1 to 12.2 Ma (Figure 4-2). From 12.2 to 10.1 Ma the ε_{Nd} values become more variable, ranging from -5.6 to 0 with a minimum baseline that decreases from ~-4 to -5.6. From 10.1 to 9.0 Ma ε_{Nd} values slowly decrease to a value of ~-6.6.

The total range of ε_{Nd} values for site 999 (Colombian Basin) is from -6.4 to -0.1 (Figure 4-1, Table 4-3). From 14.0 Ma to 13.7 Ma the ε_{Nd} values increase from -5.5 to -3.1 (Figure 4-2). Values remain around ~-3.0 from 13.7 to 12.1 Ma. At 12.0 Ma there is one point with a non radiogenic value of -6.4. After this, the ε_{Nd} values become more variable. From 12.0 to 10.6 Ma the ε_{Nd} values range from -3.0 to -0.1, and from 10.6 to 10.2 Ma values demonstrate a smaller range of variability range from -3.0 to -4.4. The ε_{Nd} values shift to more radiogenic values of ~-2.0 from 10.2 to 9.4 Ma, and then decrease to -6.0 from 9.4 to 9.1 Ma. The final point at 9.0 Ma increases to -4.8.

4.2 ε_{Nd} Compared to Carbonate MAR

The records for site 998 and 999 have been broken down into five intervals (pre-crash, pre-crash transition, crash, post-crash transition, and post-crash) based on the ε_{Nd} and the carbonate MAR records (Figure 4-2). During the pre-crash interval at site 998 (>13.5 Ma), the carbonate MAR and the ε_{Nd} signals are relatively steady with ε_{Nd} values around ~-4 and carbonate MAR around ~0.75. At site 999, ε_{Nd} values become more radiogenic, shifting from -5.5 to -3.1 during the pre-crash interval (>13.5 Ma), while the carbonate MAR decreases from ~2 to 1.25 g/cm^2 per k.y.

During the pre-crash transition interval (13.5 – 12 Ma), the ε_{Nd} values at sites 998 and 999 are relatively stable with values ranging between -4.3 to -3.5 and -3.7 to -2.4 respectively. The carbonate MARs at site 999 range from 0 to 1.5 g/cm^2 per k.y. and are more variable during the pre-crash transition, while, those at site 998 are relatively constant at ~1.25 g/cm^2 per k.y.

During the crash interval (12-10 Ma) the ε_{Nd} values are much more variable with values ranging from -3.9 to 0 at site 998, and from -4.4 to -0.1 at site 999. The carbonate MARs at both sites are highly variable with values as low as ~0 and as high as ~1.3 g/cm^2 per k.y. There is a general negative correlation between low carbonate MAR and radiogenic ε_{Nd} values at both sites during the crash interval.

The post-crash transition and post-crash intervals are marked by increased carbonate MAR with values around ~1.0 at both sites. At site 998, the ε_{Nd} values decrease from ~-5.5 to ~-6 over the combined sections. At Site 999, the ε_{Nd} values increase to ~-2 during the post-crash transition interval, then decrease to ~-6 during the post crash interval.

At site 846, low carbonate MAR occurs later than in the Caribbean basin, and the record has been divided into just two intervals (pre-crash and crash) because the post-crash recovery

was not recorded by this dataset and smaller subdivisions are not warranted. During the pre-crash interval (14.14 to 11.2 Ma), the ε_{Nd} values begin at -3.8 and increase to more radiogenic values around ~-2, while carbonate MARs are ~0.5 to 1.0 (Figure 4-2). During the crash interval (11.2 to 8.1 Ma) carbonate MARs are ~0 to 0.5 and ε_{Nd} values remain relatively stable ranging between ~-1.7 and -2.3 with a short shift to -2.93 at 10.6 Ma and a decrease to -2.9 at 8.09 Ma, which correlates with a brief increase in carbonate MAR. Site 846 also shows a general negative correlation between low carbonate MAR and radiogenic ε_{Nd} values during the carbonate crash interval, similar to the correlation observed at sites 998 and 999.

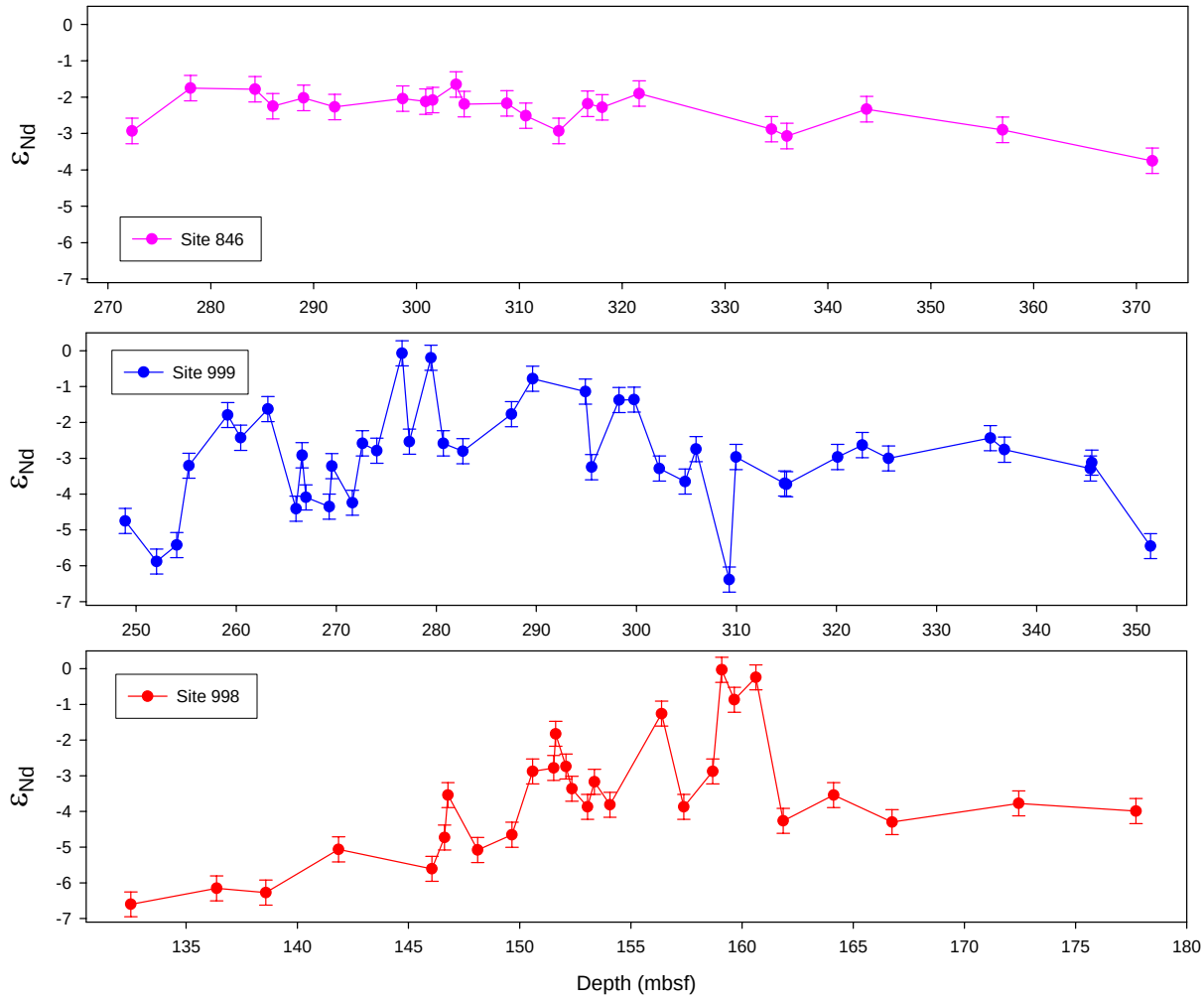

Figure 4-1. ε_{Nd} values from site 846 in the eastern equatorial Pacific, sites 999 and 998 in the Caribbean Basin plotted versus depth.

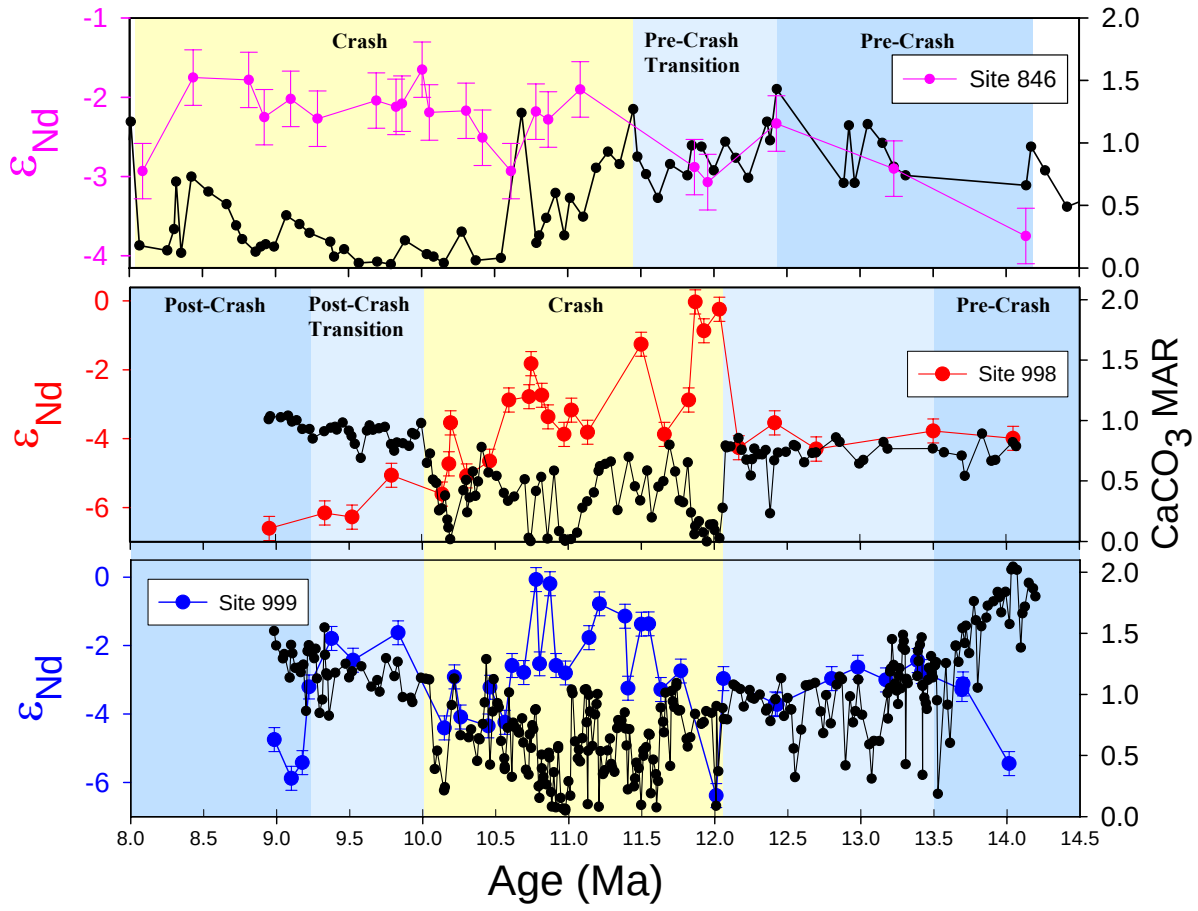

Figure 4-2. εNd values and carbonate MARs from site 846 in the eastern equatorial Pacific and sites 999 and 998 in the Caribbean Basin spanning from 8 to 14.5 Ma. Carbonate MARs for site 846 are from Farrell et al. (1995) and for sites 999 and 998 are from Roth et al. (2000). Based on carbonate MARs site 846 is divided into two intervals, pre-crash and crash, and the two Caribbean sites are divided into five intervals (pre-crash, pre-crash transition, crash, post-crash transition, and post-crash).

Table 4-1. Nd isotopes of Fossil Fish Teeth from ODP Site 846.

Sample	Depth (mbsf)	Age (Ma)	$^{143}Nd/^{144}Nd$	$\varepsilon_{Nd(o)}$	2σ
846B-29X-6W 61-67	272.34	8.09	0.512488	-2.93	0.35
846B-30X-3W 110-116	278.03	8.43	0.512549	-1.75	0.35
846B-31X-1W 77-83	284.30	8.81	0.512547	-1.78	0.35
846B-31X-2W 101-107	286.04	8.92	0.512523	-2.25	0.35
846B-31X-4W 98-104	289.02	9.10	0.512535	-2.02	0.35
846B-31X-6W 101-107	292.04	9.29	0.512529	-2.27	0.35
846B-32X-4W 103-109	298.66	9.69	0.512534	-2.04	0.35
846B-32X-6W 27-33	300.90	9.82	0.512530	-2.12	0.35
846B-32X-6W 94-100	301.57	9.86	0.512532	-2.08	0.35
846B-33X-1W 100-107	303.84	10.00	0.512554	-1.65	0.35
846B-33X-2W 31-37	304.64	10.05	0.512526	-2.19	0.35
846B-33X-4W 144-150	308.78	10.30	0.512527	-2.17	0.35
846B-33X-6W 30-36	310.63	10.42	0.512510	-2.51	0.35
846B-34X-1W 140-146	313.83	10.61	0.512488	-2.93	0.35
846B-34X-3W 121-127	316.64	10.78	0.512526	-2.18	0.35
846B-34X-4W 111-117	318.04	10.87	0.512521	-2.28	0.35
846B-34X-7W 21-27	321.64	11.09	0.512541	-1.90	0.35
846B-36X-2W 128-134	334.51	11.87	0.512491	-2.88	0.35
846B-36X-3W 128-134	336.01	11.96	0.512481	-3.07	0.35
846B-37X-2W 93-99	343.76	12.43	0.512519	-2.33	0.35
846B-38X-4W 144-150	356.98	13.23	0.512490	-2.90	0.35
846B-40X-1W 121-127	371.54	14.14	0.512446	-3.75	0.35

Table 4-2. Nd isotopes of Fossil Fish Teeth from ODP Site 998.

Sample	Depth (mbsf)	Age (Ma)	$^{143}Nd/^{144}Nd$	$\varepsilon_{Nd(o)}$	2σ
998A-15H-1W 21-26	132.51	8.95	0.512300	-6.60	0.35
998A-15H-3W 107-113	136.37	9.33	0.512323	-6.15	0.35
998A-15H-5W 27-32	138.58	9.52	0.512320	-6.27	0.35
998A-16H-1W 54-59	141.85	9.79	0.512379	-5.06	0.35
998A-16H-3W 126-129	146.05	10.14	0.512351	-5.61	0.35
998A-16H-4W 32-37	146.62	10.18	0.512396	-4.73	0.35
998A-16H-4W 45-50	146.77	10.19	0.512457	-3.54	0.35
998A-16H-5W 25.5-30	148.11	10.30	0.512378	-5.08	0.35
998A-16H-6W 32-36	149.65	10.46	0.512400	-4.65	0.35
998A-16H-6W 125-130	150.58	10.59	0.512491	-2.88	0.35
998A-17H-1W 21-26	151.53	10.73	0.512496	-2.78	0.35
998A-17H-1W 32-37	151.62	10.75	0.512545	-1.82	0.35
998A-17H-1W 77-82	152.08	10.82	0.512498	-2.74	0.35
998A-17H-1W 105-110	152.35	10.86	0.512466	-3.36	0.35
998A-17H-2W 25-30	153.05	10.97	0.512440	-3.87	0.35
998A-17H-2W 54-60	153.36	11.02	0.512476	-3.17	0.35
998A-17H-2W 126-131	154.06	11.13	0.512443	-3.81	0.35
998A-17H-4W 55-60	156.38	11.50	0.512574	-1.26	0.35
998A-17H-5W 2-7	157.38	11.66	0.512440	-3.87	0.35
998A-17H-5W 134-139	158.68	11.82	0.512491	-2.88	0.35
998A-17H-6W 26-31	159.09	11.87	0.512637	-0.03	0.35
998A-17H-6W 81-87	159.65	11.93	0.512594	-0.87	0.35
998A-17H-CCW 2-7	160.62	12.03	0.512626	-0.24	0.35
998A-18X-1W 105-111	161.85	12.17	0.512420	-4.26	0.35
998A-18X-3W 32-36	164.12	12.41	0.512457	-3.54	0.35
998A-19X-1W 53-58	166.75	12.70	0.512418	-4.30	0.35
998A-19X-5W 24-28	172.44	13.50	0.512445	-3.77	0.35
998A-20X-2W 32-36	177.72	14.05	0.512434	-3.99	0.35

Table 4-3. Nd isotopes of Fossil Fish Teeth from ODP Site 999.

Sample	Depth (mbsf)	Age (Ma)	$^{143}Nd/^{144}Nd$	$\varepsilon_{Nd(o)}$	2σ
999A-28X-1W 18-23	248.91	8.98	0.512395	-4.75	0.35
999A-28X-3W 32-36	252.04	9.10	0.512337	-5.88	0.35
999A-28X-4W 84-88	254.06	9.18	0.512360	-5.42	0.35
999A-28X-5W 55-59	255.27	9.22	0.512474	-3.21	0.35
999A-29X-1W 72-76	259.14	9.38	0.512546	-1.79	0.35
999A-29X-2W 51-57	260.44	9.52	0.512514	-2.43	0.35
999A-29X-4W 25-29	263.17	9.83	0.512555	-1.63	0.35
999A-29X-6W 5-10	265.98	10.15	0.512417	-4.31	0.35
999A-29X-6W 66-70	266.58	10.22	0.512489	-2.92	0.35
999A-29X-6W 104-109	266.97	10.26	0.512428	-4.09	0.35
999A-30X-1W 128-132	269.30	10.45	0.512415	-4.35	0.35
999A-30X-2W 3-8	269.56	10.46	0.512473	-3.22	0.35
999A-30X-3W 59-63.5	271.61	10.56	0.512421	-4.24	0.35
999A-30X-4W 8-14	272.61	10.61	0.512506	-2.58	0.35
999A-30X-5W 2-7	274.05	10.69	0.512495	-2.79	0.35
999A-30X-6W 105-110	276.58	10.78	0.512634	-0.07	0.35
999A-30X-7W 28-33	277.31	10.80	0.512508	-2.53	0.35
999A-31X-2W 34-38	279.46	10.87	0.512628	-0.19	0.35
999A-31X-3W 7-12	280.70	10.91	0.512506	-2.58	0.35
999A-31X-4W 53-59	282.66	10.98	0.512494	-2.80	0.35
999A-32X-1W 28-33	287.51	11.14	0.512547	-1.77	0.35
999A-32X-2W 90-94	289.62	11.21	0.512598	-0.78	0.35
999A-32X-6W 18-23	294.91	11.39	0.512580	-1.14	0.35
999A-32X-6W 79-84	295.52	11.41	0.512472	-3.25	0.35
999A-33X-2W 4-10	298.27	11.50	0.512568	-1.38	0.35
999A-33X-3W 4-8	299.76	11.55	0.512568	-1.37	0.35
999A-33X-4W 106-111	302.29	11.63	0.512470	-3.29	0.35
999A-33X-6W 65-69	304.87	11.72	0.512455	-3.56	0.35
999A-33X-CCW 13-18	305.96	11.77	0.512501	-2.67	0.35
999A-34X-2W 145-150	309.28	12.01	0.512308	-6.44	0.35
999A-34X-3W 63-67	309.95	12.06	0.512486	-2.96	0.35
999A-34X-6W 100-105	314.83	12.41	0.512448	-3.70	0.35
999A-34X-6W 118-122	315.00	12.43	0.512447	-3.72	0.35
999A-35X-3W 109-113	320.11	12.80	0.512486	-2.96	0.35
999A-35X-5W 54-59	322.57	12.98	0.512503	-2.63	0.35
999A-35X-7W 17-21	325.19	13.17	0.512484	-3.00	0.35
999A-37X-1W 15-19	335.37	13.19	0.512513	-2.44	0.35
999A-37X-2W 6-11	336.79	13.42	0.512497	-2.76	0.35
999A-38X-1W 55-60	345.38	13.69	0.512470	-3.29	0.35
999A-38X-1W 69-73	345.51	13.70	0.512478	-3.12	0.35
999A-38X-5W 55-60	351.38	14.01	0.512359	-5.45	0.35

CHAPTER 5
DISCUSSION

5.1 The Source of Caribbean Basin ε_{Nd} Values in the Middle/Late Miocene

The ε_{Nd} values within the Caribbean Basin extend to values that are more radiogenic than any known intermediate/deep water masses within the equatorial Atlantic region. A critical question is whether these values represent the true water mass signature or a diagenetic product. An obvious source of radiogenic Nd is Caribbean arc volcanism. During the time interval of this study, the Caribbean Basin was influenced by volcanic ash deposition with an ε_{Nd} value of ~+7 (Drummond et al., 1995). Abundant layers and disseminated ash are observed at site 998 (Yucatan Basin) and site 999 (Colombian Basin) (Peters et al., 2000). However, a plot of the low resolution ash MAR versus ε_{Nd} for these sites illustrates that there is no correlation between intervals of abundant ash and samples with more radiogenic ε_{Nd} values (Figure 5-1). Another possible diagenetic input would be sediment from the Magdalena and Orinoco Rivers in South America that drain into the Caribbean Basin. The Magdalena River sediment has an ε_{Nd} value of -8.3 (Goldstein et al., 1984), while the Orinoco River sediment has an ε_{Nd} value of ~-14 (Goldstein et al., 1997). Thus, these values are far too negative to have generated the radiogenic ε_{Nd} values observed in the Caribbean Basin.

Although the ε_{Nd} values in the Caribbean are distinct from those in the Atlantic, they are very similar to values recorded in the Pacific today and during the Miocene (Ling et al., 1997; O'Nions et al., 1998; Frank et al., 1999; Reynolds et al., 1999; van de Flierdt et al., 2004). Values for Pacific intermediate waters in the Miocene range from -3.6 to -4.0 from 9.2 to 13.4 Ma in the western equatorial Pacific (Fe-Mn crust D11-1, 11º39'N, 161º41'E, 1,870-1,690m; Ling et al., 1997), from 9.9 to 14.5 Ma in the central equatorial Pacific (Fe-Mn crust CD29-2, 16º42'N, 168º14'W, 2,390-1,970m; Ling et al., 1997), and from -2.0 to -2.6 from 8.8 to 13.13

Ma in the north Pacific (Fe-Mn crusts 13D-27A and D4-13A, Kamchatka and Alaska, 1,500 and 2,100 m; van de Flierdt et al., 2004) (Figure 5-2). The distribution of ε_{Nd} in modern water column profiles from the western north Pacific illustrates a similar range of values. Surface waters from 3 m in this region have an ε_{Nd} value of -0.1, while deep waters at 4,481 m have an ε_{Nd} value of -3.9 (Piepgras and Jacobsen, 1988). A second profile near a Fe-Mn crust studied by van de Flierdt et al. (2004) documents a similar range of ε_{Nd} values with +0.3 at 30 m and -4.5 at 2,800m (Piepgras and Jacobsen, 1988). van de Flierdt et al. (2004) concluded that in addition to becoming less radiogenic with depth, the ε_{Nd} values in the Pacific become more radiogenic at progressively higher latitudes in the North Pacific.

The correlation between values recorded in the Caribbean and Pacific, plus associated shifts in stable isotope data (Figures 5-3 and 5-4) support the idea that the ε_{Nd} values in the Caribbean Basin during the middle/late Miocene are dominated by a signature from the Pacific; indicating that throughflow in the CAS was predominantly from west to east. Benthic $\delta^{13}C$ values have been used as a proxy for deep ocean circulation based on the fact that $\delta^{13}C$ decrease along the pathway of the global conveyor (i.e., Savin et al., 1981; Curry and Lohman, 1982; Kroopnick, 1985; Woodruff and Savin, 1989; Broecker et al., 1990; Charles and Fairbanks, 1992); however, this proxy also responds to carbon cycling. Roth et al. (2000) showed that middle to late Miocene $\delta^{13}C$ values shifted from 0.1 to 1.4‰ in the Caribbean, and, like the ε_{Nd} values, the $\delta^{13}C$ values became more variable throughout the crash interval (Figure 5-3 and 5-4). Charles and Fairbanks (1992) showed modern $\delta^{13}C$ values of intermediate water in the equatorial Pacific fall within the range of <0‰ to 0.8‰, while intermediate water in the equatorial Atlantic have values >0.7‰; however, the distinction between the Pacific and Atlantic was more subtle during the Miocene (Wright and Miller, 1996; Poore et al., 2006).

Nd isotopes provide a mechanism for deconvolving the circulation and nutrient signals inherent in $\delta^{13}C$. Piotrowski et al. (2005) used plots of ε_{Nd} and $\delta^{13}C$ in the Southern Ocean to illustrate that there are correlated shifts between the two systems, which they attributed to changes driven by circulation and water mass composition on long-term and millennial timescales. They also noted a lead/lag relationship during glacial terminations, indicating that changes in $\delta^{13}C$, and therefore the carbon mass balance of the ocean, preceded changes in circulation as represented by ε_{Nd} . A similar comparison between ε_{Nd} and $\delta^{13}C$ for the Caribbean sites illustrates a general correlation between the two records, supporting the idea that the variations in ε_{Nd} record changes in circulation rather than ash diagenesis (Figures 5-3 and 5-4).

The radiogenic ε_{Nd} values observed at sites 998 and 999 do not support the original interpretation by Roth et al. (2000) that the waters filling the Caribbean during the middle to late Miocene were derived from AAIW or NAIW. Instead, the ε_{Nd} values are similar to Pacific intermediate waters (Figure 5-2). This flow of Pacific water from west to east through the CAS is also predicted by several general ocean circulation models evaluating the effects of an open Isthmus of Panama (e.g., Mikolajewicz and Crowley, 1997; Nisancioglu et al., 2003; Nof and Van Gorder, 2003; Prange and Schultz, 2004; Klocker et al., 2005; Schneider and Schmittner, 2006; Steph et al., 2006).

Based on benthic foraminiferal assemblages, Duque-Caro (1990) suggested that initial uplift of the Isthmus of Panama to 2000 m occurred between 15.9 to 15.1 Ma (ages adjusted to Shackleton et al., 1995a) and shoaling to ~1000 m (upper bathyal depths) occurred between 12-10.2 Ma (ages adjusted to Shackleton et al., 1995a). Shoaling of the Isthmus of Panama to 1000 m resulted in the flow of Pacific waters through the CAS into the Caribbean basin in the model presented by Nisancioglu et al. (2003). The flow of Pacific water into the Caribbean Basin

agrees well with coccolith and planktonic foraminiferal assemblages (Chiasson and D'Hondt, 2000; Kameo and Sato, 2000) during this time. Site 999 (Caribbean Basin) and site 844 (eastern equatorial Pacific) recorded identical assemblages from 16.2-13.6 Ma, these assemblages began to diverge between 13.6-10.7 Ma, and finally completely distinct assemblages were identified between 10.7-9.4 Ma (Kameo and Sato, 2000). Because coccoliths live within the photic zone, the data suggest the CAS limited surface water exchange by ~10 Ma.

Foraminiferal assemblages identified from site 999 also suggest the flow of Pacific water into the Caribbean (Chiasson and D'Hondt, 2000). Chiasson and D'Hondt (2000) identified temperate-latitude foraminiferal assemblages (Globoconellids) at site 999 until ~10.7 Ma, and interpreted their presence to represent an influx of cool Pacific surface water, either the California or Peru Current system depending on the position of the ITCZ (Chiasson and D'Hondt, 2000). Flohn (1981) predicts a more northerly position of the ITCZ at this time (~10ºN) as a result of thermal asymmetry attributed to the differences in ice sheet development between the northern and southern hemispheres. Due to the weaker pole-equator temperature gradient in the northern hemisphere the ITCZ shifts to a more northern position, which Steph et al. (2006) correlate to an increase in the eastward flow of Pacific waters into the Caribbean Basin; a prediction that is consistent coccolith assemblages, foraminiferal assemblages, and ε_{Nd} records during this time.

5.2 Circulation during the Caribbean Pre-Crash and Pre-Crash Transition

During the pre-crash and pre-crash transition there are subtle differences between the ε_{Nd} values of the two Caribbean sites (Figure 4-2). Values at the southern site (site 999, Colombian Basin) increase during the pre-crash interval and reach values more radiogenic than those at Site 998 during the pre-crash transition. This shift to more radiogenic ε_{Nd} values at site 999 coincides with a gradual shift to lower carbonate MARs, suggesting a progressive influx of more corrosive

and radiogenic intermediate Pacific waters through the CAS prior to the carbonate crash. The ε_{Nd} at site 998 remains relatively stable at a value similar to middle/late Miocene upper-intermediate Pacific waters, but probably represent a mixture of Pacific and Atlantic surface waters because the Nicaragua Rise acted as a barrier to intermediate and deep water flow into the northern Caribbean Basin at this time.

Faulting of the Nicaragua Rise led to the opening of the north/south oriented Pedro Channel and the northern part of the Walton Basin (Cunningham, 1998). These channels provided a passage way for deep waters and ultimately led to the development of the Caribbean Current, which flows from the southern Caribbean into the Gulf of Mexico across the region of the Nicaragua Rise (Droxler et al., 1998). Prior to the connection between sites 998 and 999, slight differences in ε_{Nd} at the two sites suggest that intermediate waters from the Pacific influenced site 999, while a mixture of Pacific and Atlantic surface waters influenced site 998 (Figure 5-5). Following the connection by ~12 Ma (Droxler et al., 1998), the range of values observed at sites 998 and 999 become more similar by ~11.8 Ma, although there are still distinctions between the two sites.

5.3 The Caribbean Carbonate Crash

At the beginning of the crash interval the ε_{Nd} values at sites 998 and 999 diverge (Figure 5-6) with the values from 12.1 to 11.8 Ma at site 998 representing surface waters from the Pacific and the values at site 999 representing either deeper waters from the Pacific or, more likely, a mixture of intermediate waters derived from the Pacific (NPIW) and Atlantic (AAIW) (Figures 4-2 and 5-2). During this time interval, site 998 still appears to be separated from the southern Caribbean Basin by the Nicaragua Rise at an upper intermediate depth. The ε_{Nd} values merge from 11.8 to 11.5 Ma and again from 10.7 to 10.18 Ma implying a connection between the northern and southern Caribbean sites that can be attributed to foundering of the Nicaragua Rise

(Droxler et al., 1992), which also lead to the initiation of the Loop Current in the Gulf of Mexico (Mullins et al., 1987).

The history of the foundering of the Nicaragua Rise has important implications for deep circulation in the Atlantic. Prior to the late early Miocene the Caribbean Current flowed through the Havana/Matanzas Channel in western Cuba (Iturralde-Vincent et al.; 1996) into the Straits of Florida, bypassing the Gulf of Mexico (Droxler et al., 1998). The Havana/Matanzas Channel closed and the Pedro Channel opened during the late middle Miocene transition, redirecting the Caribbean Current into the Gulf of Mexico, thereby initiating the Loop Current. This flow pattern effectively increases the residence time of the water in a high evaporation region, therefore the surface water exiting the Gulf of Mexico becomes more saline, leading to high salinities in the Gulf Stream and ultimately in the surface waters of the North Atlantic. It is estimated that the Loop Current was initiated ~12-15 Ma (ages converted to Shackleton et al., 1995a) in the middle Miocene (Mullins et al., 1987).

Throughout the carbonate crash interval (12-10 Ma) the carbonate MARs, $\delta^{13}C$, and ε_{Nd} records show very erratic and large shifts at sites 998 and 999 with large decreases in carbonate MARs associated with shifts to more radiogenic ε_{Nd} values. These large shifts may represent pulses of increased Pacific water inflow during carbonate dissolution events, while a greater proportion of Atlantic inflow occurred during the intervals with less radiogenic ε_{Nd} values and enhanced carbonate preservation. The periods of increased Pacific inflow can also be linked to times of increased production of NCW (Figure 5-7 and 5-8). The interval of the carbonate crash, as defined by low carbonate MARs in the Caribbean Basin, correlates well with periods of increased NCW production from ~12.4 to 9.5 Ma as determined using $\delta^{13}C$ gradients between the Atlantic and Pacific. During times of NCW production $\delta^{13}C$ values in the North Atlantic are

higher those in the Pacific. In contrast, there is very little difference between Atlantic and Pacific $\delta^{13}C$ values when the Southern Ocean is the dominant source of deep water (Woodruff and Savin,1989; Wright and Miller, 1996; Poore et al., 2006; ages calibrated to Shackleton et al., 1995a). Based on interbasin $\delta^{13}C$ gradients, Woodruff and Savin (1989) argued for early, weak production of NCW from 14.5 to 11.4 Ma (ages updated to Shackleton et al., 1995a). After this time they proposed that strong SCW production dominated the deep Pacific and Atlantic in response to growth of the Antarctic ice cap. The 11.4 Ma age (updated to Shackleton et al., 1995a) coincides with the "silica switch" (Keller and Barron, 1983) when the primary site of siliceous ooze deposition shifted from the Atlantic to the North Pacific and Indian Oceans, which Woodruff and Savin (1989) attributed to increased NCW production . Most studies agree that early NCW was produced during parts of the late middle Miocene, but the highest production of NCW in the Miocene occurred during the late Miocene (Blanc et al., 1980; Schnitker, 1980; Miller and Fairbanks, 1985; Woodruff and Savin, 1989; Wright et al., 1991, 1992, and 1996; Wei, 1995; Wei and Peleo-Alampay, 1997).

Thomas and Via (2007) developed a Neogene Nd isotopic record at Walvis Ridge in the southeastern Atlantic Ocean to evaluate the onset of NCW production. The ε_{Nd} values at site 1262 begin to decrease at ~13 Ma with a major decrease beginning at ~10.6 Ma. Thomas and Via (2007) interpret this shift to indicate greater proportions of NCW in the southeastern Atlantic Ocean. They argue that the carbonate crash in the Caribbean and equatorial Pacific was the result of the onset of deep water formation in the Labrador Sea. The offset in the timing of the carbonate crash and the timing of the decrease in ε_{Nd} values was probably a result of a low resolution ε_{Nd} record (Thomas and Via, 2007). In the Caribbean, the Nd isotopic record agrees

with enhanced NCW production determined by Wright and Miller (1996) and Poore et al. (2006) in which they suggested was controlled by the flow over North Atlantic sills

Wright and Miller (1996) used $\delta^{13}C$ gradients between the Atlantic, Pacific and Southern Ocean to calculate the %NCW production. Poore et al. (2006) updated the %NCW production calculations using new data and found that increased NCW production occurred at ~12 Ma, which is similar to the results Wright and Miller (1996) that suggest an increase at ~12.5 Ma. A comparison between this calculated %NCW production and the ε_{Nd} record for Site 998 and 999 illustrates that, in general, increased production of NCW correlates with more radiogenic ε_{Nd} values and decreased carbonate MARs (Figure 5-7 and 5-8). In other words, the carbonate crash events occur during times of enhanced NCW production.

The overall correlation between increased ε_{Nd} values and decreased carbonate MARs can therefore be attributed to the flow of corrosive intermediate and surface Pacific waters through the CAS into the Caribbean Basin during times of enhanced NCW production. This water would then flow north across the shallow Nicaragua Rise, ultimately filling both basins (Colombian and Yucatan) with corrosive waters with radiogenic Nd isotopes.

The one exception to this correlation occurs at ~12 Ma at Site 999 when increased NCW production and decreased carbonate MARs coincides with less radiogenic ε_{Nd} values. One possible explanation is that these less radiogenic ε_{Nd} values during this early carbonate crash interval represent AAIW that flowed into the southern Caribbean basin when NCW production rates were high. Thus, the southern basin was filled with a mixture of corrosive AAIW and NPIW, with AAIW dominating at ~12 Ma, while the northern basin was filled with shallow/intermediate Pacific water (Figure 5-9). This idea is similar to the theory presented by Roth et al. (2000) that increased NCW was compensated by reduced NAIW and, therefore, more

corrosive AAIW overflowed the sills and filled the Caribbean Basin. As mentioned previously, the northern site (998) was still separated from the southern Caribbean by the Nicaragua Rise; therefore, this site records shallow/intermediate Pacific throughflow observed in subsequent crash intervals instead of the deeper NAIW/AAIW mix.

5.4 Circulation during the Caribbean Post-Crash Transition and Post-Crash

The ε_{Nd} values at sites 998 and 999 diverge during the post-crash transition. Site 999 records a brief excursion to more radiogenic ε_{Nd} values from 9.8 to 9.4 Ma, while site 998 continues to shift to less radiogenic values. The timing of these events correlates with a decrease in NCW production (Wright and Miller, 1996; Poore et al., 2006) (Figures 5-7 and 5-8), and a shift to light $\delta^{13}C$ after the Caribbean carbonate MAR recovered (Figures 5-3 and 5-4). The brief excursion at site 999 records more Pacific-like values, while Site 998 continues to record an Atlantic/Pacific value with a decreasing Pacific component (Figure 5-10). The lack of a dissolution event associated with radiogenic ε_{Nd} values at site 999 could have been the result of increased productivity and an associated increase in the carbonate rain rate in response to an increase in nutrient levels supplied from old, Pacific waters. The $\delta^{13}C$ values recorded at site 999 (Roth, 1998) supports with this interpretation because the values become lighter, indicating a more nutrient-rich water mass filling the southern Caribbean Basin (Figure 5-4). The fact that site 998 ε_{Nd} values decrease while site 999 ε_{Nd} values increase also supports the idea that at least part of the $\delta^{13}C$ signal is a response to productivity rather than water mass. An alternative scenario is that the entire Caribbean was filled with more Atlantic sourced water (i.e. NAIW) as a result of the decreasing production of NCW, but site 999 continued to record more radiogenic ε_{Nd} values because of its proximal location to the CAS. The mixture of upper NPIW, Pacific surface waters, and NAIW at this site would account for the combination of enhanced carbonate preservation and more radiogenic ε_{Nd} values. The continual decrease in ε_{Nd} values at site 998

during this time suggests that the mixture observed at site 999 combined with a progressively increasing fraction of Atlantic waters before circulating into the northern basin.

Gradually decreasing ε_{Nd} values during the post-crash transition and post-crash at site 998 and post-crash at site 999 highlight the gradual reduction of Pacific throughflow coincident with the shoaling of the Isthmus of Panama and the foundering of the Nicaragua Rise. Frank et al. (1999) and Reynolds et al. (1999) proposed a decrease in Pacific throughflow entering the Florida Straits via the Loop Current beginning at ~8.5 Ma based on data from Fe-Mn crusts in the equatorial Pacific and Florida Straits. Data from sites 998 and 999 illustrate that decreasing throughflow began at ~10.7 Ma. It is impossible to determine whether the Atlantic source at this time was NAIW or AAIW because the percentage of Pacific versus Atlantic inflow is unknown.

5.5 The Pacific Carbonate Crash

Shoaling of the Isthmus of Panama and the subsequent production of NCW also affected circulation patterns in the Pacific Ocean and contributed to the middle Miocene carbonate crash in the eastern equatorial Pacific, although this event at site 846 lags the crash in the Caribbean Basin. The idea is that enhanced NCW production resulted in a greater contribution of NCW to Circumpolar Water (CPW), thereby lengthening the pathway of deep water entering the Pacific and resulting in older, more corrosive deep waters. In today's ocean much of the Pacific deep water flows southward as either NPIW or PCW (Mix, Tiedemann, Blum, et al., 2003; Figure 5-11). The formation of NPIW occurs with relatively little interaction with the atmosphere, causing the water mass to remain depleted in oxygen, high in CO_2 (Talley, 1993), and have the highest nutrient concentration in the Pacific (Figure 5-11). Enhanced global conveyor circulation associated with NCW production would therefore result in more corrosive NPIW, PCW, and North Pacific Surface and increased flow of that water toward the south.

The ε_{Nd} shift toward slightly more radiogenic values during the carbonate crash interval at site 846 (Figure 4-2) supports this link between NCW production and the composition of Pacific waters. More radiogenic ε_{Nd} values and decreased carbonate MAR's would both result from the expansion of corrosive NPIW and PCW southward in response to NCW production. The timing of dissolution events recorded at sites in the eastern equatorial Pacific documents the development and introduction of this more corrosive water mass from the north. The most northerly site examined in the eastern equatorial Pacific (Leg 138 site 845; 3,715 m) experienced a large decrease in carbonate MARs beginning at approximately 12 Ma. Carbonate dissolution also occurred between ~12 to 9 Ma at an intermediate water depth site (Leg 202 site 1241 on the Coccos Ridge; 2,027 m) at the same latitude as the CAS (Mix, Tiedemann, Blum, et al., 2003). Sites 844 (3,415 m) and 846 (3,307 m) on the other hand, which are further south than site 845, did not begin to experience carbonate dissolution until ~11.5 Ma. Thus, the introduction of corrosive waters coming from the north Pacific progressed from the more northerly sites to more southerly sites.

The carbonate MAR and ε_{Nd} records for site 846 suggest that this site does not represent the endmember of the intermediate depth water flowing into the Caribbean Basin. Instead, it monitors the water mass that flowed south of the CAS into the Peru Basin. On the other hand, site 1241 located on the Coccos Ridge across from the CAS in the Pacific at intermediate depth might be a better site to monitor the Pacific intermediate depth throughflow because of its location and depth.

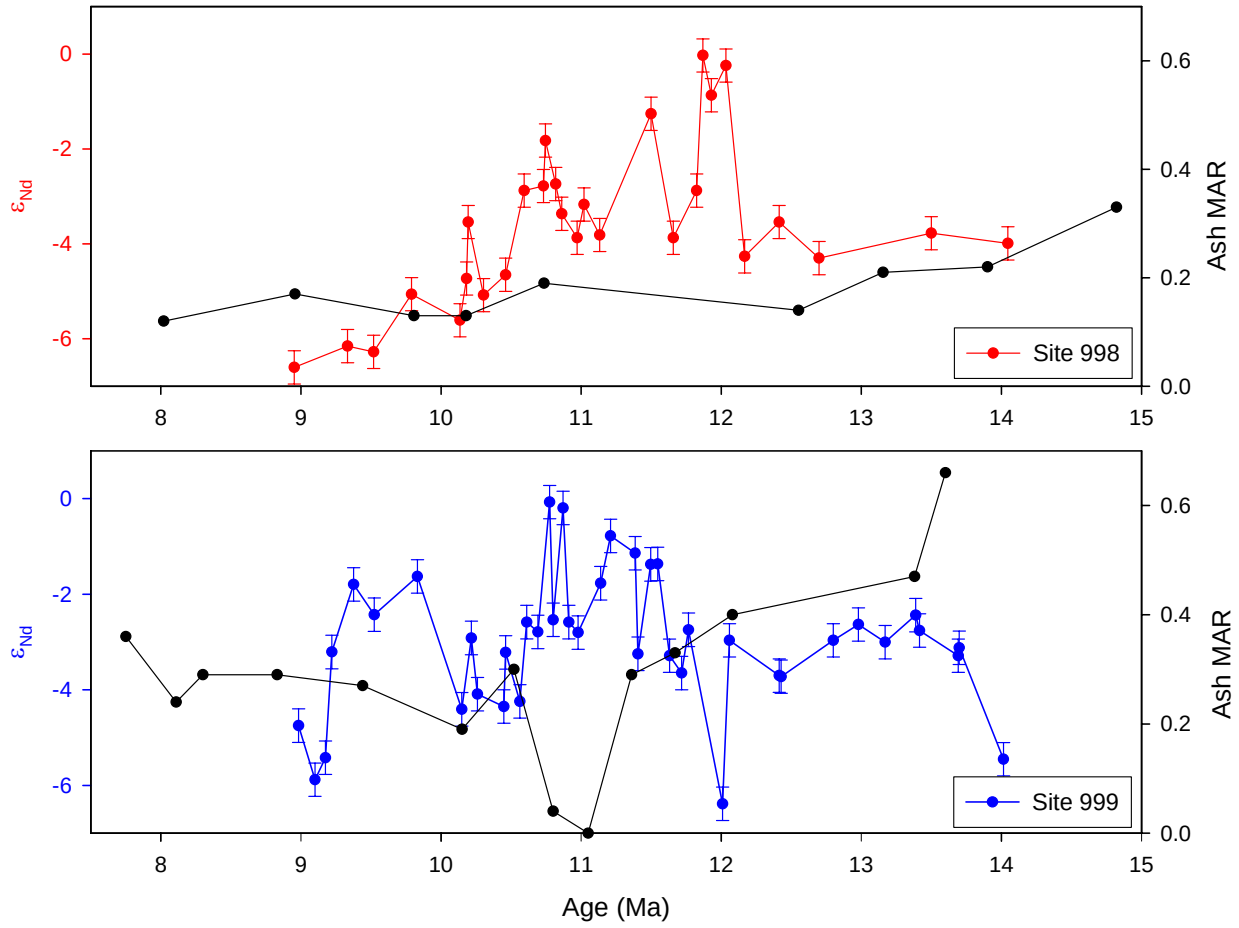

Figure 5-1. ε_{Nd} values and ash MARs (Peters et al., 2000) from sites 999 and 998 in the Caribbean Basin spanning from 8 to 14.5 Ma.

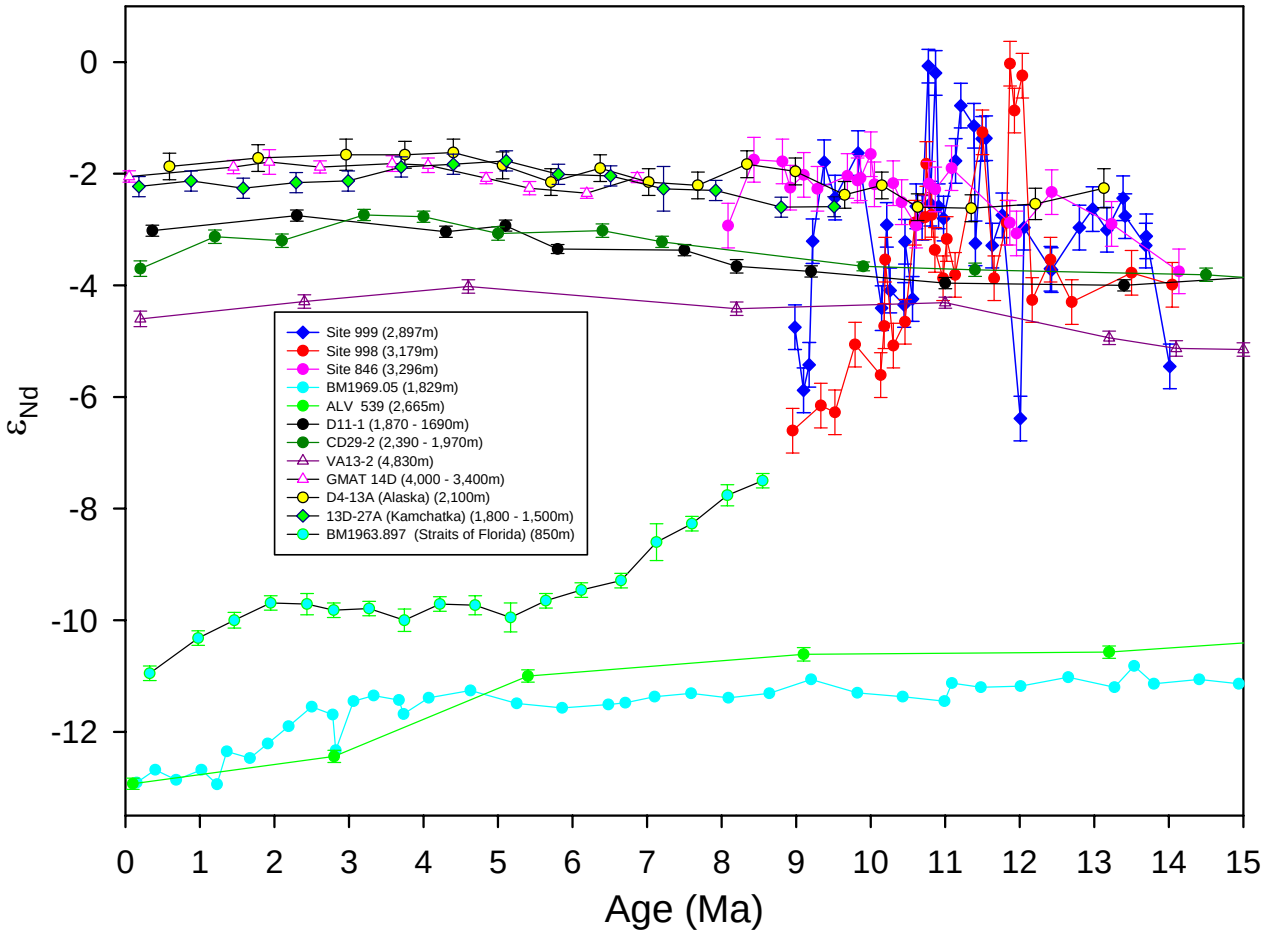

Figure 5-2. ε_{Nd} values from sites 998 and 999 in the Caribbean Basin, site 846 in the eastern equatorial Pacific, Fe-Mn crusts from the North Atlantic, Straits of Florida, North Pacific, central equatorial Pacific (Burton et al., 1997, 1999 (BM1969.05); O'Nions et al., 1998 (ALV 539)), Straits of Florida (Reynolds et al., 1999 (BM1963.897)), North Pacific (van de Flierdt et al., 2004 (D4-13A, 13D-27A)), central equatorial Pacific (Ling et al., 1997 (VA13-2, CD29-2, D11-1); Frank et al., 1999 (GMAT 14D)). ε_{Nd} values from sites 998 and 999 are very similar to Pacific values from 14 to ~10 Ma. Following the carbonate crash they approach values recorded at BM1963.897 in the Straits of Florida.

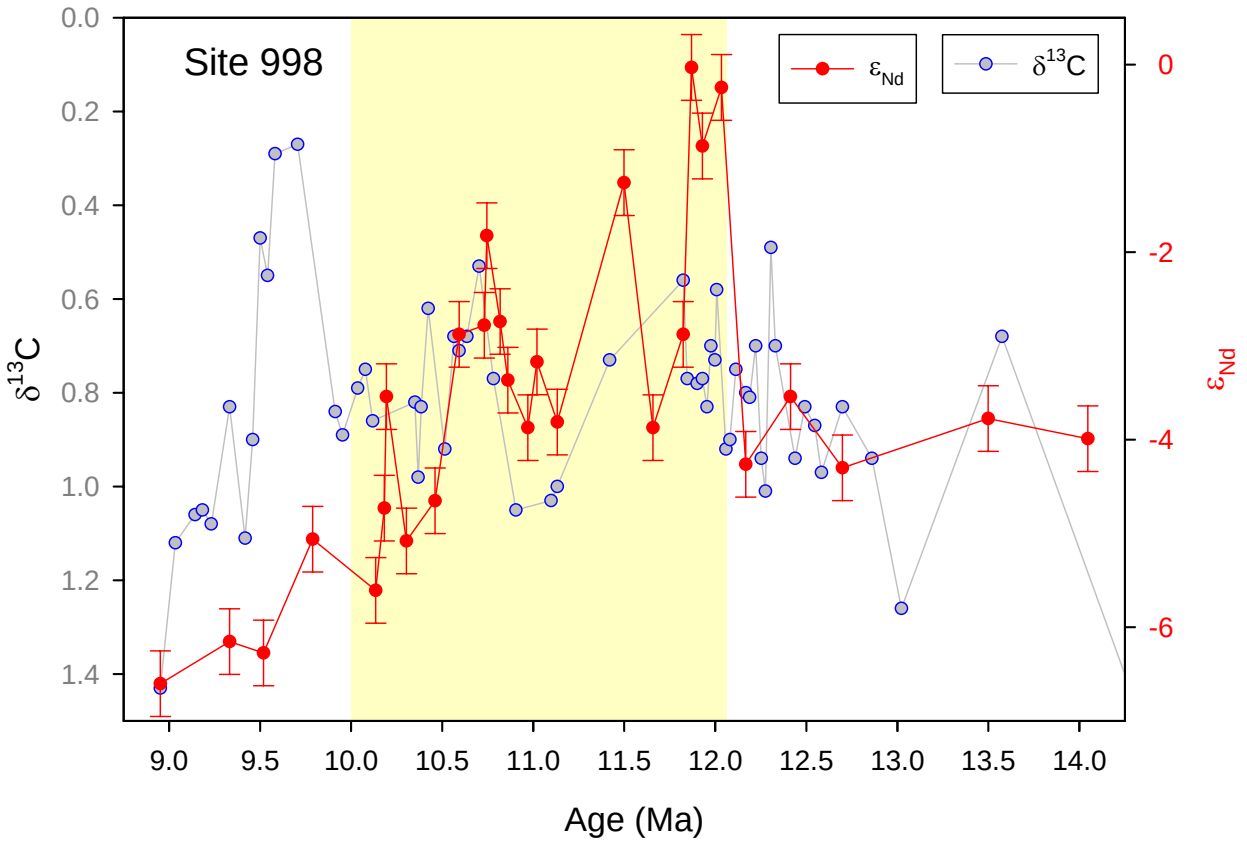

Figure 5-3. ε_{Nd} and $\delta^{13}C$ values (Roth, 1998) from site 998.

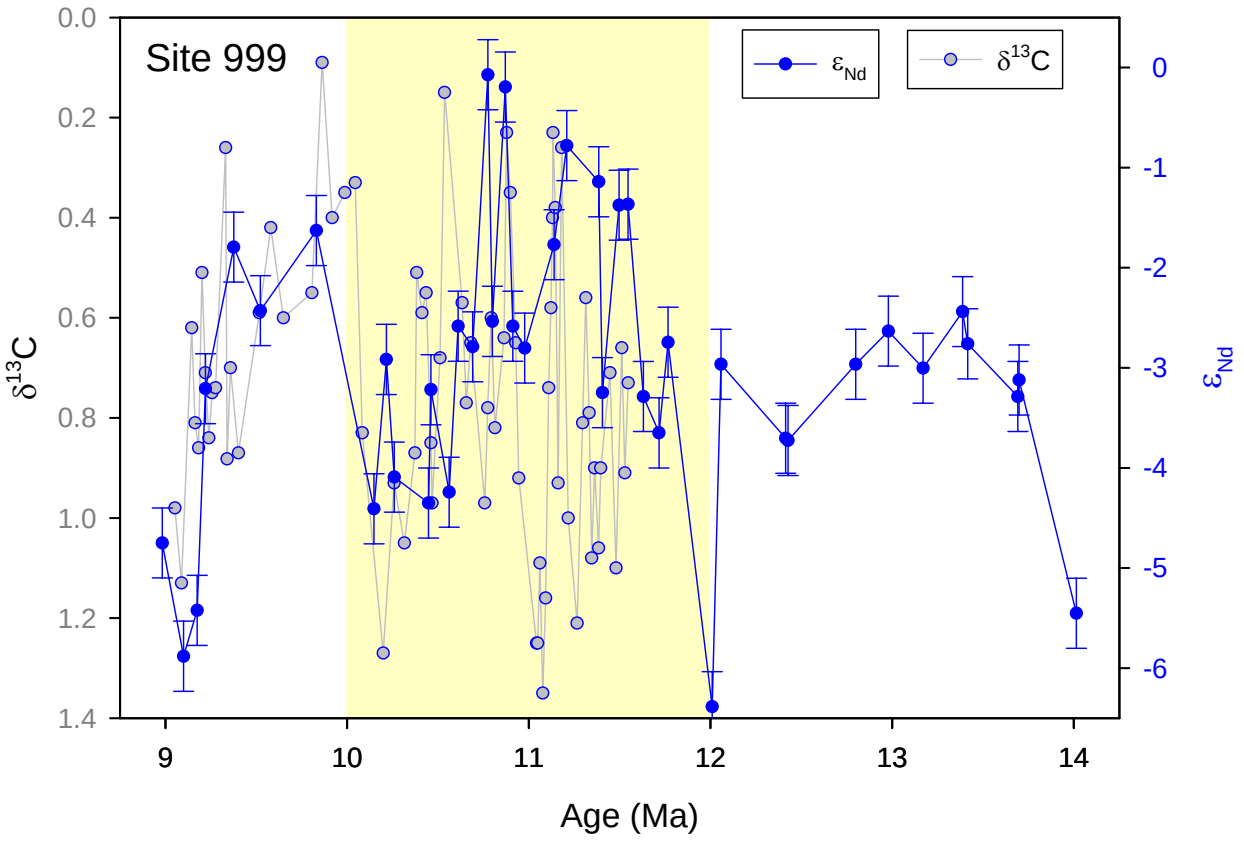

Figure 5-4. ε_{Nd} and $\delta^{13}C$ values (Roth, 1998) from site 999.

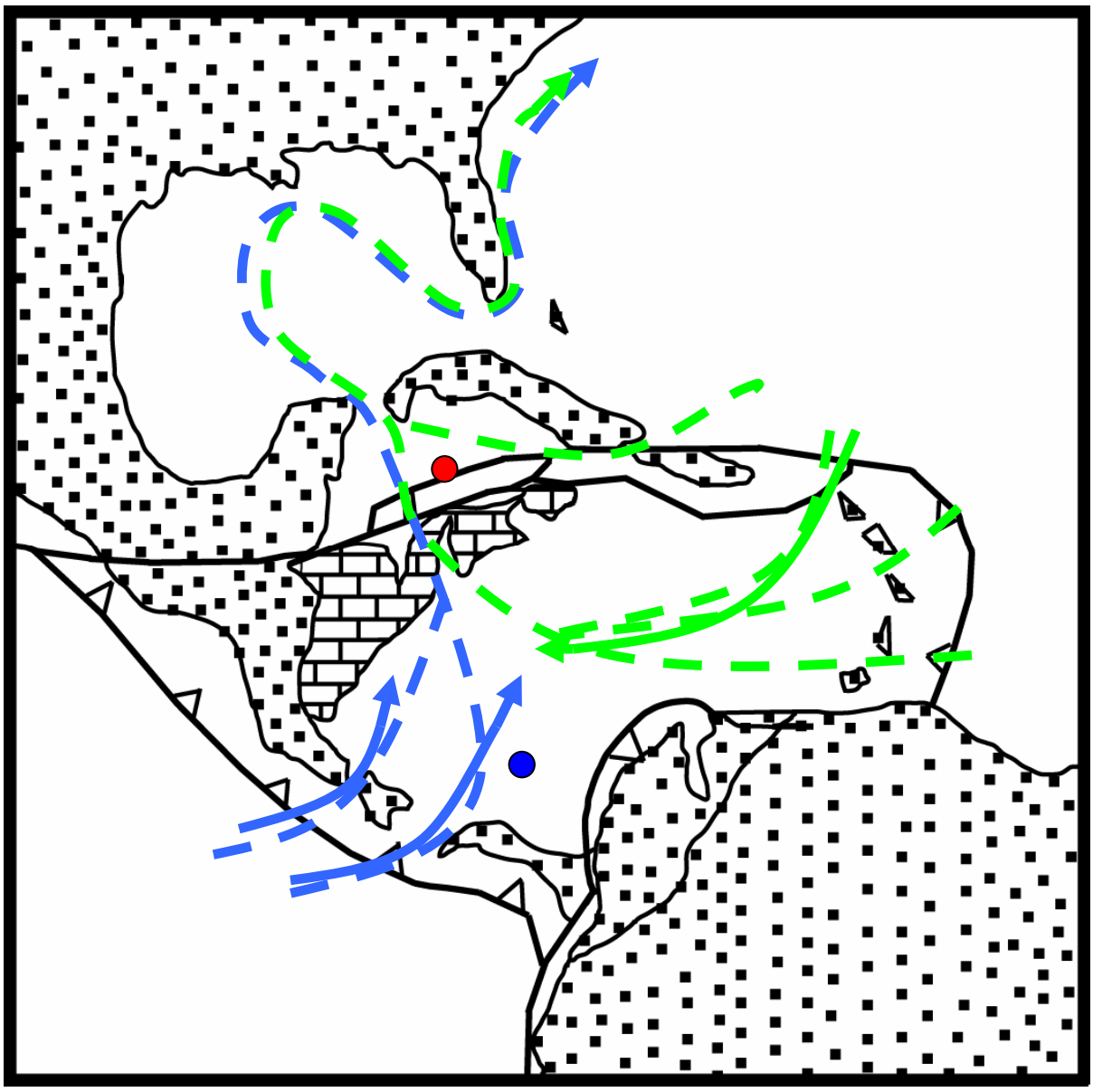

Figure 5-5. Flow patterns of Atlantic (green) and Pacific (blue) waters during the Pre-Crash/Pre-Crash Transition intervals. Solid lines represent flow of intermediate water and dashed lines represent upper/surface flow. Simplified reconstruction of the Caribbean Basin (after Pindell (1994) and modified from Roth et al. (2000)).

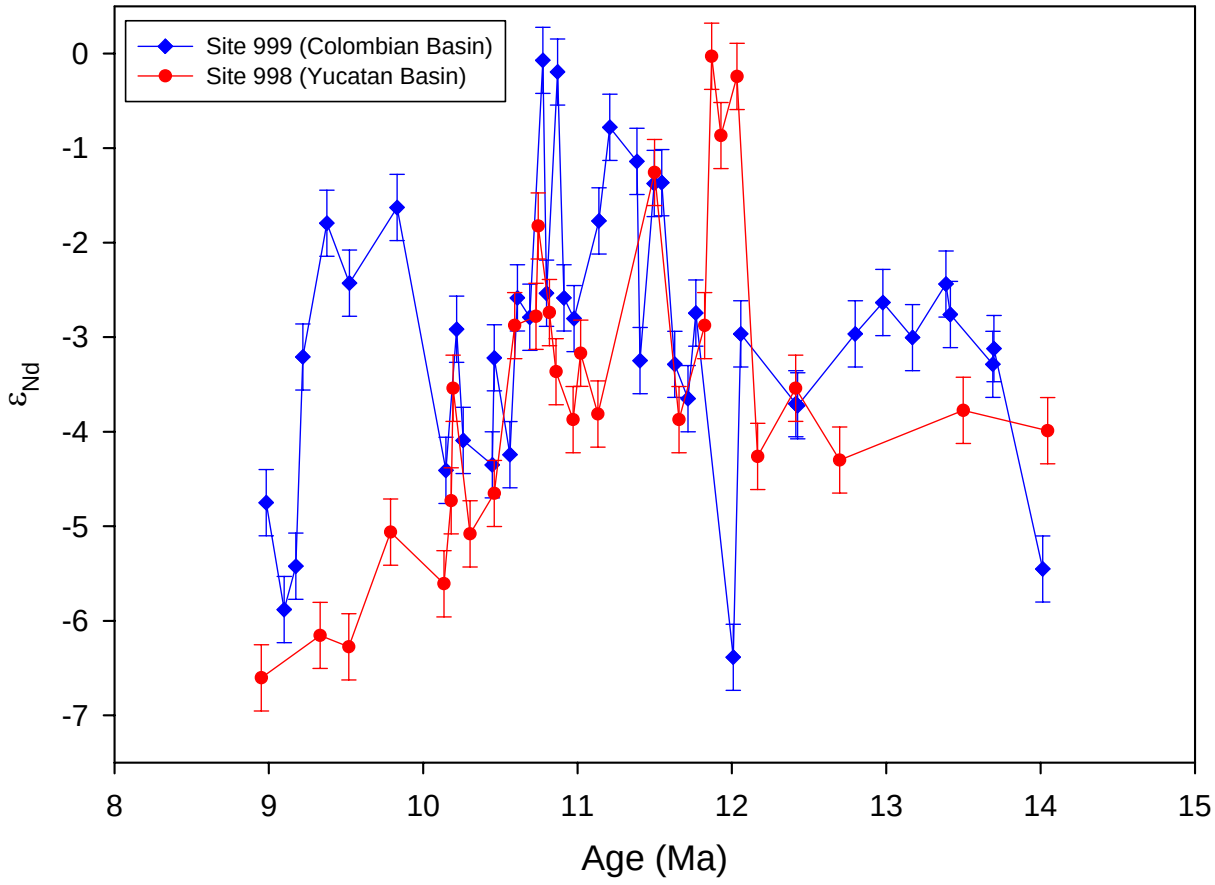

Figure 5-6. ε_{Nd} values from sites 998 and 999 in the Caribbean Basin spanning from 8 to 14.5 Ma.

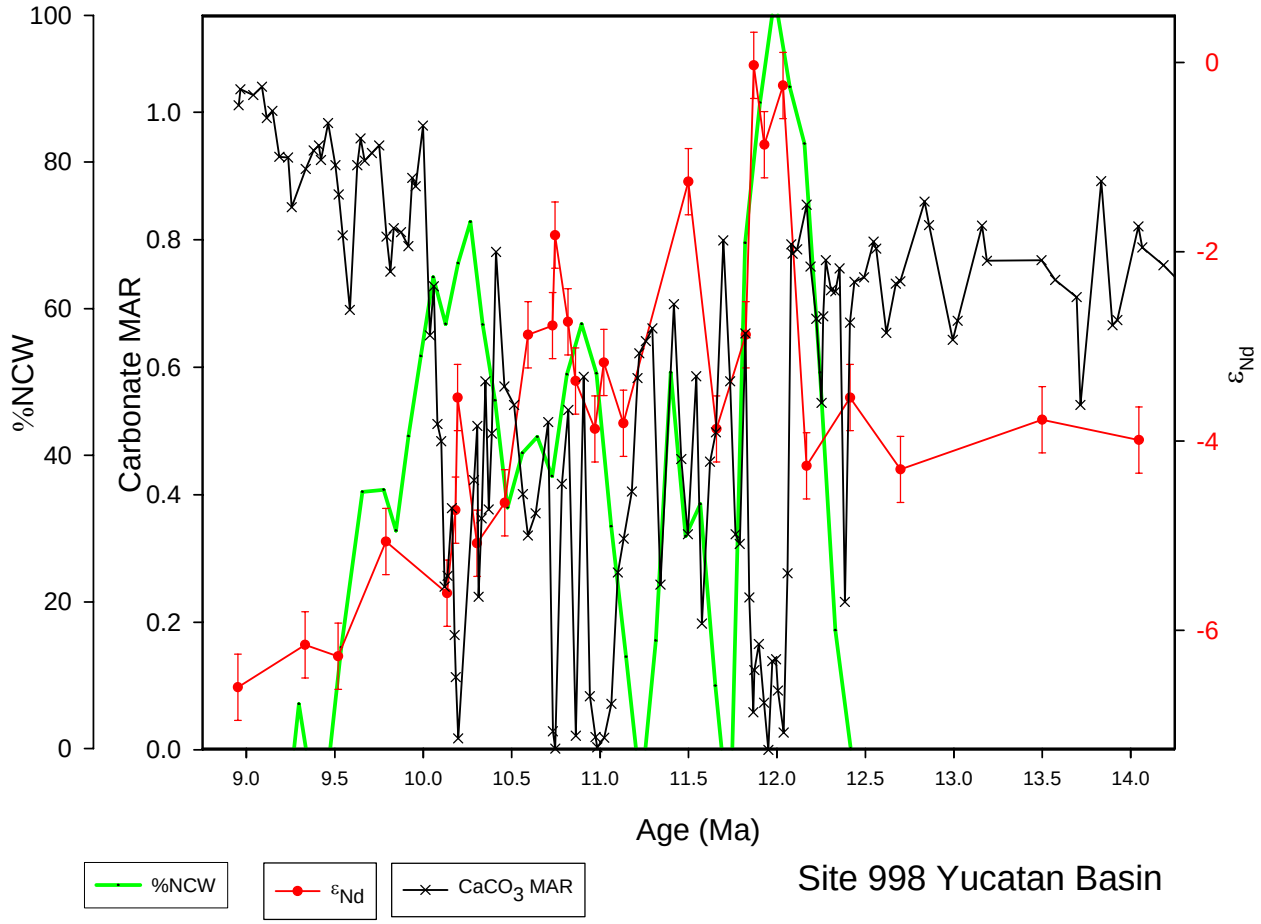

Figure 5-7. ε_{Nd} values from site 998, carbonate MAR (Roth et al., 2000), and %NCW (Wright and Miller, 1996).

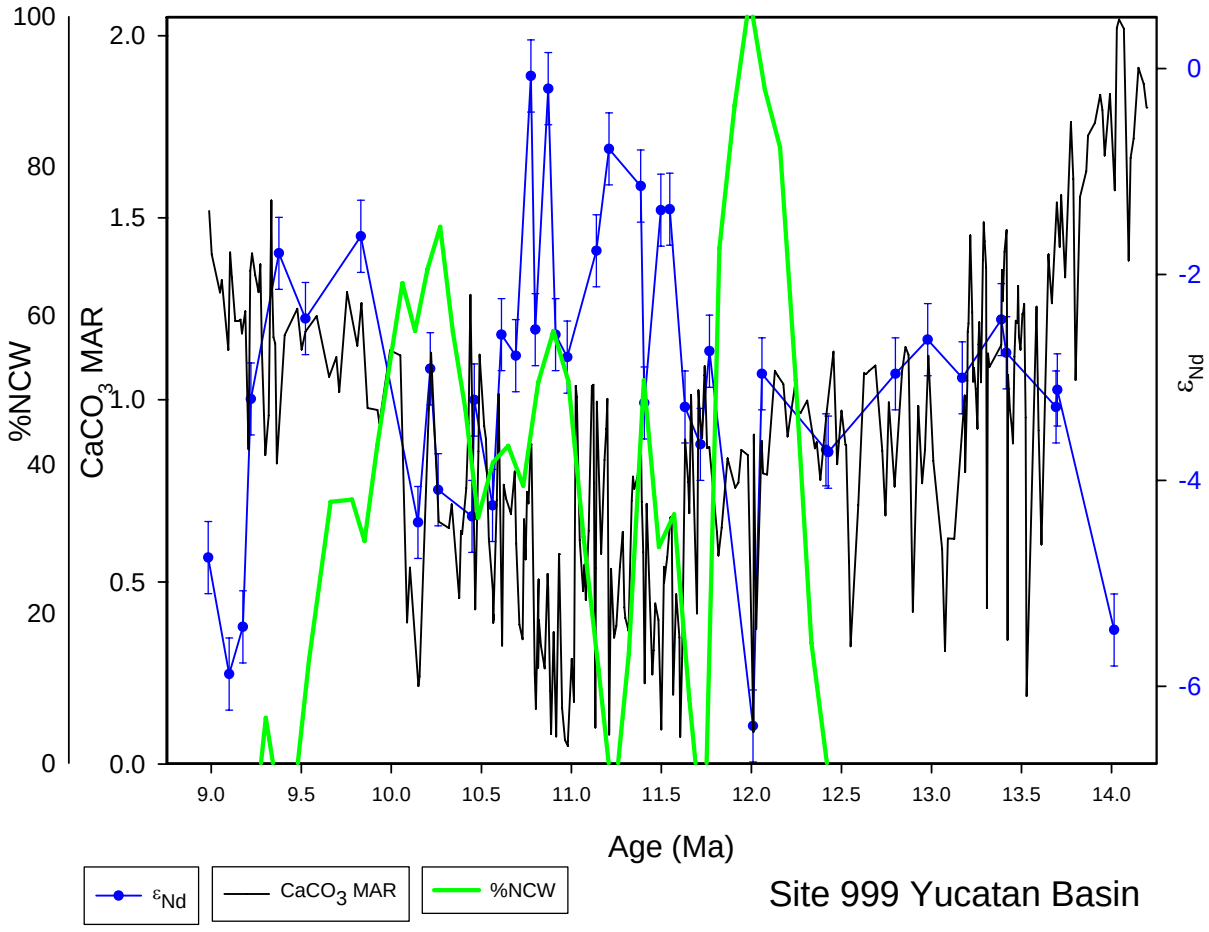

Figure 5-8. ε_{Nd} values from site 999, carbonate MAR (Roth et al., 2000), and %NCW (Wright and Miller, 1996).

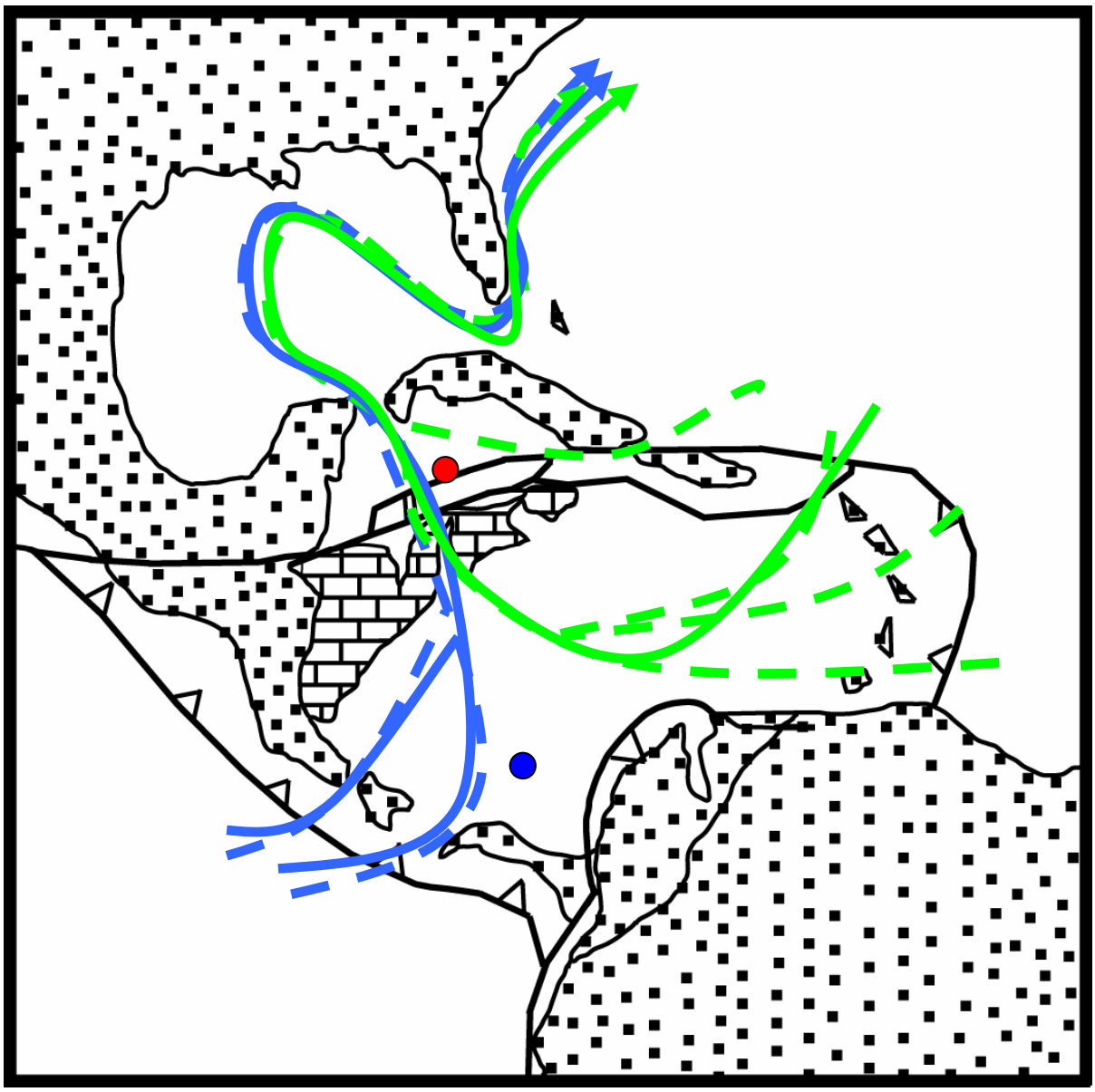

Figure 5-9. Flow patterns of Atlantic (green) and Pacific (blue) waters during the Carbonate Crash interval. Solid lines represent flow of intermediate water and dashed lines represent upper/surface flow. Simplified reconstruction of the Caribbean Basin (after Pindell (1994) and modified from Roth et al. (2000)).

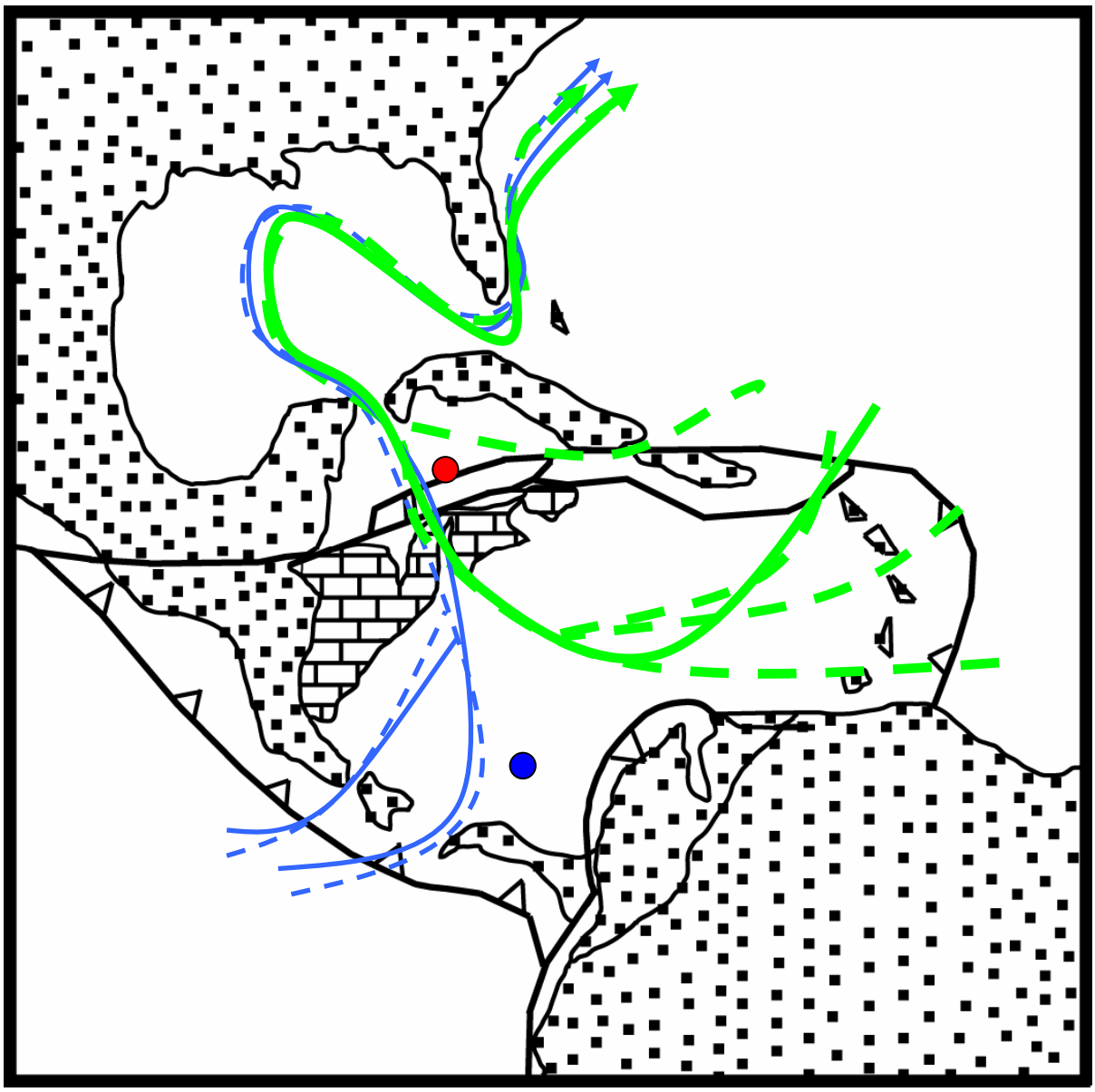

Figure 5-10. Flow patterns of Atlantic (green) and Pacific (blue) waters during the Post-Crash Transition/Post-Crash intervals. Solid lines represent flow of intermediate water and dashed lines represent upper/surface flow. Simplified reconstruction of the Caribbean Basin (after Pindell (1994) and modified from Roth et al. (2000)).

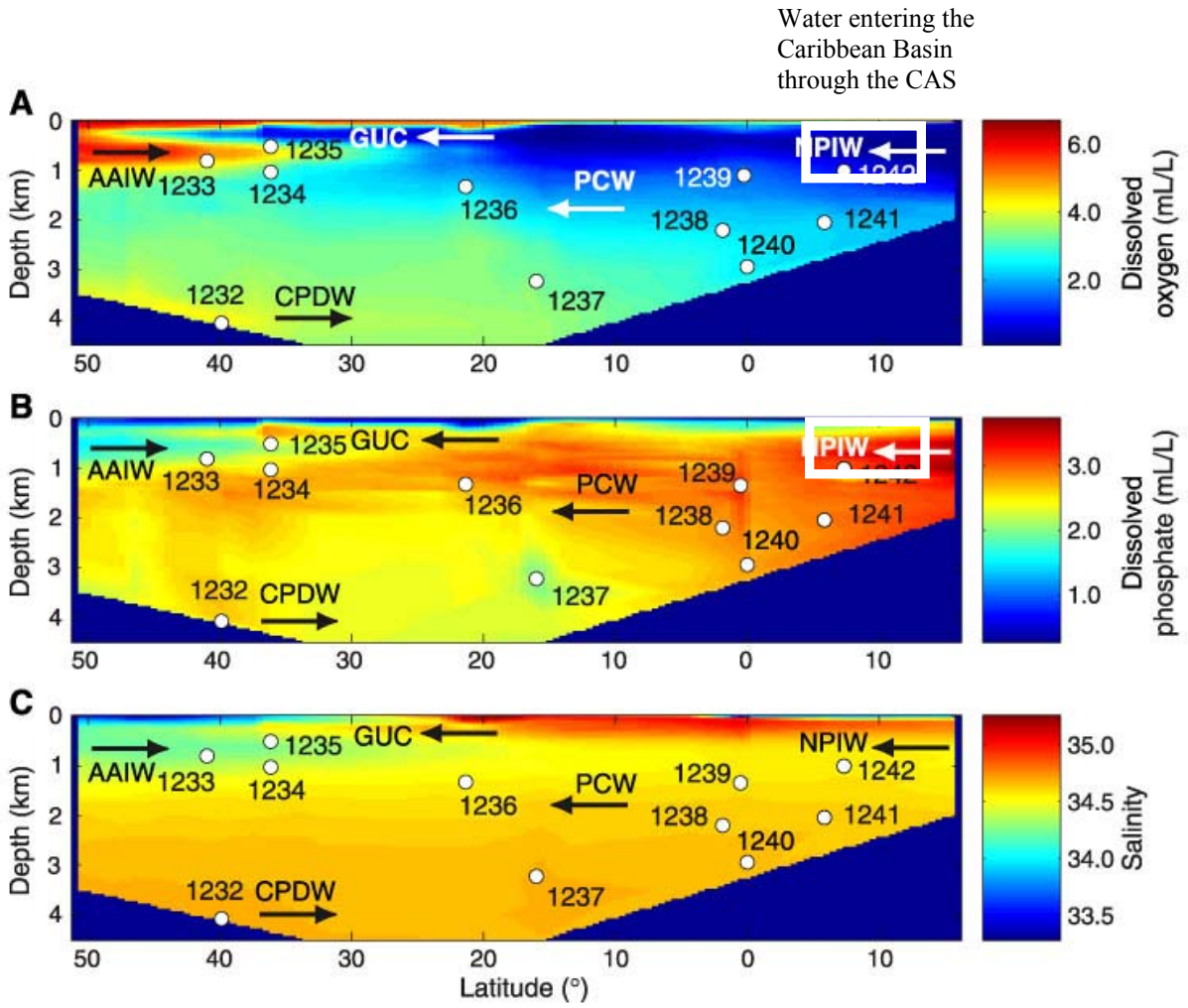

Figure 5-11. Dissolved oxygen profile from the Pacific (modified after Mix, Tiedemann, Blum, et al., 2003). White box indicates the water mass which would flow through the CAS after the Isthmus of Panama shoaled to 1000 m.

CHAPTER 6
CONCLUSIONS

Fossil fish teeth were analyzed from sites 998 and 999 in the Caribbean Basin and site 846 in the eastern equatorial Pacific to study ocean circulation using Nd isotopes during the middle to late Miocene carbonate crash. The radiogenic ε_{Nd} values recorded in the Caribbean Basin range from 0 to -6.6 and are distinct from values reported in the Atlantic. The lack of correlation between ε_{Nd} and ash deposition in the Caribbean Basin and the close correlation to values recorded in the Pacific during the Miocene argue that these radiogenic values represent CAS throughflow rather than ash alteration. West to east flow through the CAS is consistent with general ocean circulation models and $\delta^{13}C$ data.

In the Caribbean Basin, more radiogenic ε_{Nd} values correlate with intervals of decreased carbonate MARs. The gradual decrease in carbonate MARs and increase in ε_{Nd} values beginning at ~14 Ma at site 999 indicates the gradual introduction of a more corrosive, intermediate water mass flowing into the southern Caribbean Basin from the Pacific, while the northern Caribbean Basin site (site 998) ε_{Nd} values and carbonate MARs remained relatively stable with values representing a mixture of Pacific and Atlantic surface waters. During the carbonate crash interval (12-10 Ma) the ε_{Nd} values are highly variable and peak at 0 ε_{Nd} units, indicating pulses of Pacific waters entering the Caribbean Basin. This inflow of Pacific waters into Caribbean Basin through the CAS is predicted by several GCMs looking at the affects of CAS sill depths, NADW production, and the location of the ITCZ.

Although sites 998 and 999 record similar ε_{Nd} values there are distinct differences between the two records that can be attributed to their locations relative to the CAS, as well as the extent of communication across the Nicaragua Rise. After the carbonate crash, the ε_{Nd} values in the Caribbean gradually shift to less radiogenic values, indicating a gradual decline in the amount of

Pacific water entering the Caribbean Basin, coincident with the shoaling of the Isthmus of Panama. The increased proportion of Atlantic waters in the water mass exiting the Caribbean and flowing through the Straits of Florida is also documented by decreasing ε_{Nd} values in an Fe-Mn crust from the Straits of Florida (Reynolds et al., 1999).

Site 846 in the Pacific shows a similar pattern to the Caribbean Basin in which the ε_{Nd} values shift to more radiogenic values during times of decreased carbonate MARs. The initiation of the Pacific carbonate crash appears to be the result of the continued shoaling of the Isthmus of Panama and enhanced production of NCW. The increase in the ε_{Nd} to more NPIW values, and the southward progression of low carbonate MARs from sites 845 and 1251 to sites 844 and 846 farther south support the idea that older, more corrosive NPIW and PCW flowed southward in the eastern equatorial Pacific, causing the carbonate crash in this region.

Wright and Miller (1996) and Poore et al. (2006) suggest increased NCW production was the result of the subsidence of the Greenland-Scotland Ridge in the North Atlantic. These results also indicate that increased NCW production coincides with shoaling of the Isthmus of Panama, foundering of the Nicaragua Rise, and the carbonate crash in the Caribbean region. In the Caribbean region, foundering of the Nicaragua Rise and the development of the Loop Current increased the residence time of waters in the Gulf of Mexico resulting in more saline outflow to the North Atlantic, further enhancing NCW production. In addition, enhanced production of NCW affected the age of CDW flowing into the Pacific Ocean, resulting in more corrosive NPIW and PCW returning southward, producing a north to south progression of carbonate dissolution from the eastern equatorial Pacific region and Caribbean Basin to the southern eastern equatorial Pacific region during the middle/late Miocene carbonate crash.

LIST OF REFERENCES

Abouchami W., Goldstein S.L.., Galer S.J.G., Eisenhauer A., and Mangini A. (1997) Secular changes of lead and neodymium in central Pacific seawater recorded by a Fe-Mn crust. *Geochim. Cosmochim. Acta* **61**(18), 3957-3974.

Albarede F., and Goldstein S.L. (1992) World map of Nd isotopes in sea-floor ferromanganese deposits. *Geology* **20**, 761-763.

Albarede F., Goldstein S.L., and Dautel D. (1997) $^{143}Nd/^{144}Nd$ of Mn nodules from the Southern Ocean and Indian oceans, the global oceanic Nd budget, and their bearings on the deep ocean circulation during the Quaternary. *Geochim. Cosmochim. Acta* **61**, 1277-1291.

Austin J. A., Schlager W., Palmer A.A., and ODP Leg 101 Scientific Party. (1988) Proceedings of the Ocean Drilling Program, Initial Reports (Part A). Ocean Drilling Program, College Station, Texas.

Belshaw N. S., Freedman P.A.., O'Nions R.K.., Frank M., and Guo Y. (1998) A new variable dispersion double-focusing plasma mass spectrometer with performance illustrated for Pb isotopes. *International Journal of Mass Spectrometry* **181** 51-58.

Bertram C. J., and Elderfield H. (1993) The geochemical balance of the rare earth elements and Nd isotopes in the oceans. *Geochim. Cosmochim. Acta* **57**, 1957-1986.

Bird D., Hall S. A., Casey J.F., and Millegan P.S. (1993) Interpretation of magnetic anomalies over the Grenada Basin. *Tectonics* **12**, 1267-1279.

Blanc P.-L.., Rabussier D., Vergnaud-Grazzini C., and Duplessy J.C. (1980) North Atlantic Deep Water formed by the later middle Miocene. *Nature* **283**, 553-555.

Boyle E. A. (1981) Cadmium, Zinc, Copper and Barium in foraminifera tests. *Earth Planet. Sci. Lett.* **53**, 11-35.

Boyle E. A., and Kiegwin L.D. (1985) Comparison of Atlantic and Pacific paleochemical records for the past 215,000 y: Changes in deep ocean circulation and chemical inventories. *Earth Planet. Sci. Lett.* **76**, 135-150.

Broecker W.S., and Peng T.-H. (1982) *Tracers in the Sea*. Eldigio Press.

Broecker W. S., Bond G., Klaus M., Bonani G.A., and Wolfli W. (1990) A salt oscillator in the glacial Atlantic? 1. The concept. *Paleoceanography* **5**, 469-477.

Buckry D. (1973) Low-latitude coccolith biostratigraphic zonation. In: Edgar N.T., Saunders J.B., et al. (Ed.),*Init. Repts. DSDP 15*. U.S. Govt. Printing Office, Washington. 685-703

Burton K. W., Ling H.-F., and O'Nions R.K. (1997) Closure of the Central American Isthmus and its effect on deep-water formation in the north Atlantic. *Nature* **386**, 382-385.

Burton K.W., Lee D.-C., Christensen J.N., Halliday A.N., and Hein J.R. (1999) Actual timing of neodymium isotopic variations recorded by Fe-Mn crusts in the western North Atlantic. *Earth Planet. Sci. Lett.* **171**, 149-156.

Charles C.D., and Fairbanks R.G. (1992) Evidence from Southern Ocean sediments for the effect of North Atlantic deep-water flux on climate. *Nature* **355**, 416-419.

Chiasson W.P., and D'Hondt S.L.. (2000) Neogene Planktonic Foraminifer Biostratigraphy at Site 999, Western Caribbean Sea. In: Leckie, R. M., Siquardssom, H., Acton, G.D., and Draper, G. (Ed.),*Proc. ODP, Sci. Res. 165*. Ocean Drilling Program, College Station, TX.

Coates A.G., Jackson J.B., Collins L.S., Cronin T.M., Dowsett H.J., Bybell L.M., Jung P., and Obando J.A. (1992) Closure of the Isthmus of Panama: the near-shore marine record of Costa Rica and Western Panama. *Geol. Soc. Am. Bull.* **104**, 814-828.

Cunningham A. D. (1998) Neogene Evolution of the Pedro Channel Carbonate System, Northern Nicaragua Rise [Ph.D. thesis], Rice University.

Curry W.B., and Lohmann G.P. (1982) Carbon isotopic changes in benthic foraminifera from the western South Atlantic: Reconstruction of glacial abyssal circulation patterns *Quaternary Research* **18**, 218-235.

Denny W.M., Austin J.A., and Buffler R.T. (1994) Seismic stratigraphy and geologic history of mid-Cretaceous through Cenozoic rocks, Southern Straits of Florida. *AAPG Bulletin* **78**, 461-487.

DePaolo D.J., and Wasserburg, G.J. (1976) Nd isotopic variations and petrogenetic models. *Geophys. Res. Lett.* **3**, 249-252.

Droxler A.W., Cunningham A.D., Hine A.C., Hallock P., Duncan D., Rosencrantz E., Buffler R., and Robinson E. (1992) Late Middle (?) Miocene segmentation of an Eocene-early Miocene carbonate megabank on the northern Nicaragua Rise. *EOS, Transactions (supplement)* **73**.

Droxler A.W., Burke K.C., Cunningham A.D., Hine A.C., Rosencrantz E., Duncan D.S., Hallock P., and Robinson E. (1998) Caribbean constraints on circulation between

Atlantic and Pacific Oceans over the past 40 million years. In: Crowley, T. J., and K.C. Burke (Ed.),*Tectonic Boundary Conditions for Climate Reconstructions*. Oxford Univ. Press, New York.

Drummond M.S., Bordelon M., De Boer J.Z.., Defant M.J., Bellon H., and Feigenson M.D. (1995) Igneous petrogenesis and tectonic settin of plutonic and volcanic rocks of the Cordillera De Talamanca, Costa Rica-Panama, Central American Arc. *American Journal of Science* **195**, 875-919.

Duque-Caro H. (1990) Neogene stratigraphy, paleoceanography and paleobiogeography in northwest South America and the evolution of the Panama Seaway. *Palaeogeogr., Palaeoclim., Palaeoecol.* **77**, 203-234.

Elderfield H., and Greaves M.J. (1982) The rare earth elements in seawater. *Nature* **296**, 214-219.

Elderfield H., and Pagett R. (1986) Rare earth elements in icthyoliths: Variations with redox conditions and depositional environments. *Sci. Total Environ.* **49**, 175-197.

Elderfield H. (1988) The oceanic chemistry of the rare earth elements. *Philos. Trans. R. Soc. London* **Ser. A**(325), 105-126.

Exon N., Kennett J.P., and Scientific Shipboard Party. (2002) Drilling reveals climatic consequences of Tasmanian Gateway opening. *EOS, Transactions AGU* **83**, 253-259.

Farrell J.D., Raffi I., Janecek T.R., Murray D.W., Levitan M., Dadey K.A., Emeis K.-C., Lyle M., Flores J. –A., and Hovan S. (1995) Late Neogene sedimentation patterns in the eastern equatorial Pacific Ocean. In *Proceeding ODP, Scientific Results*, Vol. 135 (ed. L. A. M. N.G. Pisias, and T.R. Janecek), pp. 717-756.

Frank M., and O'Nions R.K. (1998) Sources of Pb for the Indian Ocean ferromanganese crusts: a record of Himalayan erosion? *Earth Planet. Sci. Lett.* **158**, 121-130.

Flohn H. (1981) A hemispheric circulation assymetry during late Tertiary. *Geol. Rundsch.* **70**, 725-736.

Frank M., Reynolds B.C., and O'Nions R.K. (1999) Nd and Pb isotopes in Atlantic and Pacific water masses before and after closure of the Panama gateway. *Geology* **27**, 1147-1150.

Frank M., Whiteley N., Kasten S., Hein J.R., and O'Nions R.K. (2002) North Atlantic Deep Water export to the Southern Ocean over the past 14 Myr: Evidence from Nd and Pb isotopes in ferromanganese crusts. *Paleoceanography* **17**(doi:10.1029/2000PA000606).

Frank M. (2002) Radiogenic isotopes: tracers of past ocean circulation and erosional input. *Reviews in Geophysics* **40**, 1-38.

Frank M., van de Flierdt T., Halliday A.N., Kubik P.W., Hattendorf B., and Gunther D. (2003) Evolution of deepwater mixing and weathering inputs in the central Atlantic Ocean over the past 33 Myr. *Paleoceanography* **18**.

German C.R., Klinkhammer G.P., Edmond J.M., Mitra A., and Elderfield H. (1990) Hydrothermal scavenging of rare-earth elements in the ocean. *Nature* **345**, 516-518.

Goldstein S.L., O'nions R.K., and Hamilton P.J. (1984) A Sm-Nd isotopic study of atmospheric dusts and particulates from major river systems. *Earth Planet. Sci. Lett.* **70**, 221-236.

Goldstein S.J., and Jacobsen S.B. (1988) Rare earth elements in river waters. *Earth Planet. Sci. Lett.* **89**, 35-47.

Goldstein S.L., Arndt N.T., and Stallard R.F. (1997) The history of a continent from U-Pb ages of zircons from Orinoco River sand and Sm-Nd isotopes in Orinoco basin river sediments. *Chemical Geology* **138**, 271-186.

Goldstein S.L., and Hemming S.R. (2003) Long-lived isotopic tracers in oceanography, paleoceanography and ice sheet dynamics. In *Treatise on Geochemistry*, Vol. 6 (ed. H. Elderfield), pp. 453-489. Elsevier.

Gomberg D. (1974) Geology of the Portales Terrace. *Florida Science* **37**, 15.

Greaves M.J., Statham P.J., and Elderfield H. (1994) Rare earth element mobilization from marine atmospheric dust into seawater. *Marine Chemistry* **46**, 255-260.

Haddad G.A. (1994) Calcium carbonate dissolution patterns at intermediate water depths of the Tropical oceans during the Quaternary [Ph.D. thesis], Rice University.

Haddad G.A., and Droxler A.W. (1996) Metastable CaCO3 dissolution at intermediate water depths of the Caribbean and western North Atlantic: Implications for intermediate water circulation during the past 200,000 years. *Paleoceanography* **11**, 701-716.

Haug G.H., and Tiedemann R. (1998) Effect of the formation of the Isthmus of Panama on Atlantic Ocean thermohaline circulation. *Nature* **393**, 673-676.

Henry F., Jeandel C., and Minster J, -F. (1994) Particulate and dissolved Nd in the western Mediterranean Sea: Sources, fates and budget. *Marine Chemistry* **45**, 283-305.

Iturralde-Vinent M., Hubbell G., and Rojas R. (1996) Catalogue of Cuban fossil Elasmobranchii (Paleocene to Pliocene) and paleogeographic implications of their Lower to Midddle Miocene occurrence. *J. Geological Soc. Jamaica* **31**, 7-21.

Jeandel C. (1993) Concentration and isotopic compositions of Nd in the South Atlantic Ocean. *Earth Planet. Sci. Lett.* **117**, 581-591.

Jeandel C., Bishop J.K., and Zindler A. (1995) Exchange of Nd and its isotopes between seawater small and large particles in the Sargasso Sea. *Geochim. Cosmochim. Acta* **59**, 535-547.

Jeandel C., Thouron D., and Fieux M. (1998) Concentrations and isotopic compositions of neodymium in the eastern Indian Ocean and Indonesian Straits. *Geochim. Cosmochim. Acta* **62**, 2597-2607.

Johns W.E., Townsend T.L., Fratantoni D.M., and Wilson W.D. (2002) On the Atlantic inflow to the Caribbean Sea. *Deep-Sea Research I* **49**, 211-243.

Kameo K., and Bralower T.J. (2000) Neogene nannofossil biostratigraphy of Sites 998, 999, and 1000. In *Proc. ODP, Sci. Res.*, Vol. 165 (ed. R. M. Leckie, Siquardssom, H., Acton, G.D., and Draper, G.), pp. 3-18.

Kameo K., and Sato T. (2000) Biogeography of Neogene calcareous nannofossils in the Caribbean and the eastern equatorial Pacific-floral response to the emergence of the Isthmus of Panama. *Marine Micropaleontology* **39**, 201-218.

Keigwin L.D. (1982) Isotopic Paleoceanography of the Caribbean and East Pacific: Role of Panama Uplift in Late Neogene Time. *Science* **217**, 350-353.

Keller G., and Barron J.A. (1983) Paleoceanographic implications of Miocene deep-sea hiatuses. *Geol. Soc. Am. Bull.* **94**, 590-613.

Keller G., Zenker C.E., and Stone S.M. (1989) Late Neogene history of the Pacific-Caribbean gateway. *Journal of South American Earth Science* **2**, 73-108.

Kennett J.P., Houtz R.E., Andrews P.B., Edwards A.R., Gostin V.A., Hajos M., Hampton M.A., Jenkins D.G., Margolis S.V., Ovenshine A.T., and Perch-Nielsen K. (1974) Development of the Circum-Antarctic Current. *Science* **18**, 144-147.

Kennett J.P. (1977) Cenozoic evolution of Antarctic Glaciation, the Circum-Antarctic Ocean and their impact on global paleoceanography. *Journal of Geophysical Research* **82**, 3843-3860.

King T.A., Ellis Jr. W.G., Murray D.W., Shackleton N.J., and Harris S. (1997)

Miocene evolution of carbonate sedimentation at the Ceara Rise: a multivariate date/proxy approach. In *Proc. ODP, Scientific Results*, Vol. 154 (ed. N. J. Shackleton, Curray, W.B., Richter, C., and Bralower, T.J.), pp. 349-366.

Klocker A., Prange M., and Schulz M. (2005) Testing the influence of the Central American Seaway on orbitally forced Northern Hemisphere glaciation. *Geophys. Res. Lett.* **32**, L03703.

Kroopnick P. M. (1985) The distribution of ^{13}C in the world oceans. *Deep Sea Research* **32**, 57-84.

Lacan F., and Jeandel C. (2001) Tracing Papua New Guinea imprint on the central Equatorial Pacific Ocean using neodymium isotopic compositions and Rare Earth Element patterns. *Earth Planet. Sci. Lett.* **186**, 497-512.

Le J., Mix A.C., and Shackleton N.J. (1995) Late Quaternary paleoceanography in the eastern equatorial Pacific Ocean from planktonic foraminifers: a high-resolution record from Site 846. In: Pisias, N. G., Mayer L.A., Janecek T.R., Palmer-Julson A., and van Andel T.H. (Ed.),*Proc. ODP Sci. Res. 138*. Ocean Drilling Program, College Station, TX.

Lewis J.F., and Draper G. (1990) Geology and tectonic evolution of the northern Caribbean margin. In: Dengo, G., and J.E. Case (Ed.),*The Geology of North America*. The Geological Society of America, Boulder, Colo.

Ling H.-F., Burton K.W., O'Nions R.K., Kamber B.S., von Blankenburg F., Gibb A.J.,and Hein J.R. (1997) Evolution of Nd and Pb isotopes in Central Pacific seawater from ferromanganese crusts. *Earth Planet. Sci. Lett.* **146**, 1-12.

Lyle M., Dadey K.A., and FarrellJ.W. (1995) The late Miocene (11-8 Ma) eastern Pacific carbonate crash: Evidence for reorganization of deep-water circulation by the closure of the Panama Gateway. In *Proceedings ODP, Scientific Results*, Vol. 138 (ed. L. A. M. N.G. Pisias, and T.R. Janecek), pp. 821-838.

Martin E.E., and Haley B.A. (2000) Fossil fish teeth as proxies for seawater Sr and Nd isotopes. *Geochim. Cosmochim. Acta* **64**, 835-847.

Martin E.E., and Scher H. (2004) Preservation of seawater Sr and Nd in fossil fish teeth: bad news and good news. *Earth Planet. Sci. Lett.* **220**, 25-39.

Martin E.E., Macdougall J.D., Herbert T.D., Paytan A., and Kastner M. (1995) Sr and Nd isotopic analyses of marine barite separates. *Geochim. Cosmochim. Acta* **59**, 1353-1361.

Martini E. (1971) Standard Tertiary and Quaternary calcareous nannoplankton zonation. In: Farinacci, A. (Ed.),*Proc. 2nd Planktonic Conf. Roma*, Rome.

Mayer L., Pisias N., Janecek T., et al. (1992) *Proceeding of the Ocean Drilling Program, Initial Reports*. Ocean Drilling Program, College Station, TX.

Michard A.., Albarede F., Michard G., Minster J.F., and Charlou J.L. (1983) Rare-earth elemetns and uranium in high-temperature solutions from East Pacific Rise hydrothermal vent field (13-degrees-N). *Nature* **303**, 795-797.

Mikolajewicz U., and Crowley T.J. (1997) Response of a coupled ocean/energy balance model to restricted flow through the Central American isthmus. *Paleoceanography* **12**, 429-441.

Miller K.G., and Fairbanks R.G. (1985) Oligocene to Miocene carbon isotope cycles and abyssal circulation changes. In: Sundquist, E. T., and W.S. Broecker (Ed.),*The Carbon Cycle and Atmospheric CO2: Natural variations Archean to Present*. Geophys. Monogr. Ser., AGU, Washington, DC.

Mix A.C., Tiedemann R., Blum P., et al. (2003) *Proceedings of the Ocean Drilling Program, Initial Reports*. Ocean Drilling Program, College Station, TX.

Moore Jr. T.C., Shackleton N.J., and Pisias N.G. (1993) Paleoceanography and the diachrony of radiolarian events in the eastern equatorial Pacific. *Paleoceanography* **8**, 567-586.

Müller-Karger F.E., McClain C.R., Fisher T.R., Esaias W.E., and Varela R. (1989) Pigment distribution in the Caribbean Sea: Observations from space. *Prog. Oceanogr.* **23**, 23-64.

Mullins H.T., and Neumann A.C. (1979) Geology of the Miami Terrace and its paleoceanographic implications. *Marine Geology* **30**, 205-232.

Mullins H.T., Neumann A.C., Wilber R.J., Hine A.C., and Chinburg S.J. (1980) Carbonate sediment drifts in the northern Straits of Florida. *AAPG Bulletin* **64**, 1701-1717.

Mullins H.T., Gardulski A.F., Wise S.W., and Applegate J. (1987) Middle Miocene oceanographic event in the eastern Gulf of Mexico: Implications for seismic stratigraphic succession and Loop Current/Gulf Stream circulation. *Geol. Soc. Am. Bull.* **98**, 702-713.

Nisancioglu K.H., Raymo M.E., and Stone P.H. (2003) Reorganization of Miocene deep water circulation in response to the shoaling of the Central American Seaway. *Paleoceanography* **18**(1), 1006, doi:10.1029/2002PA000767.

Nof D., and van Gorder S. (2003) Did an open Panama Isthmus correspond to an invasion of Pacific water into the Atlantic? *J. Phys. Oceanogr.* **33**, 1324-1336.

O'Nions R.K., Frank M., von Blanckenburg F., and Ling H.-F. (1998) Secular variation of Nd and Pb isotopes in ferromanganese crusts from the Atlantic, Indian and Pacific Oceans. *Earth Planet. Sci. Lett.* **155**, 15-28.

Peters J.L., Murray R.W., Sparks J.W., and Coleman D.S. (2000) Terrigenous matter and dispersed ash in sediment from the Caribbean Sea: results from Leg 165. In: R.M. Leckie, S., H., Acton, G.D., and Draper, G. (Ed.),*Proceeding of the Ocean Drilling Program, Scientific Results* Ocean Drilling Program, College Station, TX.

Piepgras D.J., and Wasserburg G.J. (1982) Isotopic composition of neodymium in waters from the Drake Passage. *Science* **217**, 207-214.

Piepgras D.J., and Wasserburg G.J. (1985) Strontium and neodymium isotopes in hot springs on the East Pacific Rise and Guaymas Basin. *Earth Planet. Sci. Lett.* **72**, 341-356.

Piepgras D.J., and Wasserburg G.J. (1987) Rare earth element transport in the western North Atlantic inferred from Nd isotopic observations. *Geochim. Cosmochim. Acta* **51**, 1257-1271.

Piepgras D.J., and Jacobsen S.B. (1988) The isotopic composition of neodymium in the North Pacific. *Geochim. Cosmochim. Acta* **52**, 1373-1381.

Pinet B., Lajat D., Le Quellec P., and Bouysse P. (1985) Structure of Aves Ridge and Grenada Basin from multichannel seismic data. In: Mascle, A. (Ed.),*Geodynamique des Caraibes*. Editions Technip., Paris.

Piotrowski A. M., Goldstein S.L., Hemming S.R., and Fairbanks R.G. (2005) Temporal Relationships of Carbon Cycling and Ocean Circulation at Glacial Boundaries. *Science*.

Philander S.G.H., and Pacanowski R.C. (1986) A model of the season cycle in the tropical Atlantic. *J. Geophys. Res.* **91**, 14192-14206.

Poore H.R., Samworth R., White N.J., Jones S.M., and McCave I.N. (2006) Neogene overflow of Northern Component Water at teh Greenland-Scotland Ridge. *Geochemistry, Geophysics, Geosystems* **7**.

Popenoe P. (1985) Cenozoic depositional and structural history of the North Carolina margin from seismic stratigraphic analyses. In: Poag, C. W. (Ed.),*Geologic evolution of the United States Atlantic margin*. Van Nostrand Reinhold, New York.

Prange M., and Schulz M. (2004) A coastal upwelling seesaw in the Atlantic Ocean as a result of the closure of the Central American Seaway. *Geophys. Res. Lett.* **31**, L17207.

Puteanus D., and Halbach P. (1988) Correlation of Co concentration and growth rate: A method for age determination of ferromanganese crusts. *Chemical Geology* **69**, 73-85.

Raffi I., and Flores J.-A. (1995) Pleistocene through Miocene calcareous nannofossils from eastern equatorial Pacific Ocean (Leg 138). In *Proc. ODP, Sci. Res.*, Vol. 138 (ed. N.G. Pisias, L.A. Mayer, and T.R. Janecek), pp. 233-286.

Reynolds B.C., Frank M., and O'Nions R.K. (1999) Nd- and Pb- isotope time series from Atlantic ferromanganese crusts: implications for changes in provenance and paleocirculation over the last 8 Myr. *Earth Planet. Sci. Lett.* **173**, 381-396.

Roth J.M. (1998) The Caribbean carbonate crash at the middle to late Miocene transition and the establishment of the modern global thermohaline circulation [M.S. thesis], Rice University.

Roth J.M., Droxler A.W., and Kameo K. (2000) The Caribbean carbonate crash at the middle to late Miocene transition: linkage to the establishment of the modern global ocean conveyor. In *Proc. ODP, Sci. Results*, Vol. 165 (ed. R.M. Leckie, Siquardssom, H., Acton, G.D., and Draper, G.), pp. 249-273.

Savin S.M., Keller G., Douglas R.G., Killingley J.S., Shaughnessy L., Sommer M.A., Vincent E., and Woodruff F. (1981) Miocene benthic foraminiferal isotope records: A synthesis. *Marine Micropaleontology* **6**, 423-450.

Scher H.D., and Martin E.E. (2004) Circulation in the Southern Ocean during the Paleogene inferred from Nd isotopes. *Earth Planet. Sci. Lett.* **28**, 391-405.

Scher H.D., and Martin E.E. (2006) Timing and climatic consequences of the opening of Drake Passage. *Science* **312**, 428-430.

Schneider B., and Schmittner A. (2006) Simulating the impact of the Panamanian seaway closure on ocean circulation, marine productivity and nutrient cycling. *Earth Planet. Sci. Lett.* **246**, 367-380.

Schnitker D. (1980) North Atlantic oceanography as possible cause of Antarctic glaciation and eutrophication. *Nature* **284**, 615-616.

Segl M., Mangini A., Bonani G., Hofmann H.J., Nessi M., Sutter M., Wolfli W., Friedrich G., Pluger W.L., Wiechowski A., and Beer J. (1984) ^{10}Be dating of manganese crust from Central North Pacific and implications for oceanic paleocirculation. *Nature* **309**, 540-543.

Shackleton N.J., Crowhurst S., Hagelberg T., Pisias N.G., and Schneider D.A. (1995a) A new Late Neogene time scale: application to Leg 138 sites. In *Proc. ODP, Sci. Res.*, Vol. 138 (ed. N.G. Pisias, N.A. Mayer, T.R. Janecek, A. Palmer-Julson, and T.H. van Andel), pp. 73-101.

Shackleton N. J., Baldauf J.G., Flores J.-A., Iwai M., Moore Jr. T.C., Raffi I., and Vincent E. (1995b) Biostratigraphic Summary for Leg 138. In: Pisias, N. G., Mayer L.A., Janecek T.R., Palmer-Julson A., and van Andel T.H. (Ed.),*Proc. ODP, Sci. Res.* Ocean Drilling Program, College Station, TX.

Shackleton N.J., and Hall M.A. (1995) Stable isotope records in bulk sediments (Leg 138). In: N.G. Pisias, N. A. M., T.R. Janecek, A. Palmer-Julson, and T.H. van Andel (Ed.),*In Proceedings of the Ocean Drilling Program, Scientific Results*. Ocean Drilling Program, College Station, TX.

Shackleton N.J., and Hall M.A. (1997) The late Miocene stable isotope record, Site 926. In: Shackleton, N. J., Curry, W.B., Richter, C., and Bralower, T.J. (Ed.),*Proc. Ocean Drilling Prog., Scientific Results 154*.

Shackleton N.J., and Crowhurst S. (1997) Sediment fluxes based on an orbitally tuned time scale 5 Ma to 14 Ma, Site 926. In *Proc. ODP, Sci. Results*, Vol. 154 (ed. N. J. Shackleton, Curray, W.B., Richter, C., and Bralower, T.J.), pp. 69-82.

Shaw H.F., and Wasserburg G.J. (1985) Sm-Nd in marine carbonates and phosphates: Implications for Nd in seawater and crustal ages. *Geochim. Cosmochim. Acta* **54**, 2433-2438.

Sigurdsson H., Leckie R.M., Acton G.D., et al. (1997) *Proceeding of the Ocean Drilling Program, Initial Reports*. Ocean Drilling Program, College Station, TX.

Spivack A.J., and Wasserburg G.J. (1988) Neodymium isotopic composition of the Mediterranean outflow and the eastern North Atlantic. *Geochimica Cosmochimica Acta* **52**, 2762-2773.

Staudigel H., Doyle P., and Zindler A. (1985) Sr and Nd isotope systematics in fish teeth. *Earth Planet. Sci. Lett.* **76**, 45-56.

Steph S., Tiedemann R., Prange M., Groeneveld J., Nürnberg D., Reuning L., Schulz M., and Haug G.H. (2006) Changes in Caribbean surface hydrography during the Pliocene shoaling of the Central American Seaway. *Paleoceanography* **21**, PA4221.

Tachikawa K., Jeandel C., and Roy-Barman M. (1999a) A new approach to the Nd residence time in the ocean: the role of atmospheric inputs. *Earth Planet. Sci. Lett.* **170**, 433-446.

Tachikawa K., Jeandel C., Vangriesheim A., and Dupre B. (1999b) Distribution of rare earth elements and neodymium isotopes in suspended particles of the tropical Atlantic Ocean (EUMELI site). *Deep-Sea REs. I: Oceanogr. Res. Pap.* **46**, 733-755.

Tachikawa K., Athias V., and Jeandel C. (2003) Neodymium budget in the modern ocean and paleo-oceanographic implications. *Journal of Geophysical Research* **108**, 3254.

Talley L.D. (1993) Distribution and formation of North Pacific intermediate water. *Journal of Physical Oceanography* **23**, 517-537.

Thomas D.J., Bralower T.J., and Jones C.E. (2003) Nd isotopic reconstruction of Late Paleocene-Early Eocene thermohaline circulation. *Earth Planet. Sci. Lett.* **290**, 309-322.

Thomas D.J. (2004) Evidene for deep-water production in the North Pacific Ocean during the early Cenozoic warm interval. *Nature* **430**, 65-68.

Thomas D.J., and Via R.K. (2007) Neogene evolution of Atlantic thermohaline circulation: Perspective from Walvis Ridge, southeastern Atlantic Ocean. *Paleoceanography* **22**, PA2212.

van de Flierdt T., Frank M., Halliday A.N., Hein J.R., Hattendorf B., Gunther D., and Kubik P.W. (2004) Deep and bottom water export from the Southern Ocean to the Pacific over the past 38 million years. *Paleoceanography*.

Via R.K.., and Thomas D.J. (2006) Evolution of Atlantic thermohaline circulation: Early Oligocene onset of deep-water production in the North Atlantic. *Geology* **34**, 441-444.

von Blanckenburg F., and Igel H. (1999) Lateral mixing and advection of reactive isotope tracers in ocean basins: observations and mechanisms. *Earth Planet. Sci. Lett.* **169,**, 13-128.

Wei W. (1995) The initiation of North Atlantic Deep Water as dated by nannofossils. *J. Nannopl. Res.* **17**, 90-91.

Wei W., and Peleo-Alampay A. (1997) Onset of North Atlantic Deep Water as dated by nannofossils. *Proceedings-30th International Geological Congress, Marine Geology and Paleoceanography* **13**, 57-64.

Woodruff F., and Savin S.M. (1989) Miocene deepwater oceanography. *Paleoceanography* **4**, 87-140.

Wright J., Seymour R.S., and Shaw H.F. (1984) REE and Nd isotopes in conodont apatite: Variations with geological age and depositional environment. *GSA Spec. Paper* **196**, 325-340.

Wright J.D., Miller K.G., and Fairbanks R.G. (1991) Evolution of modern deepwater circulation: Evidence from the Late Miocene Southern Ocean. *Paleoceanography* **6**, 275-290.

Wright J.D., and Miller K.G. (1992) Early and middle Miocene stable isotopes: implications for deepwater circulation and climate. *Paleoceanography* **7**, 357-389.

Wright J.D., and Miller K.G. (1996) Control on the North Atlantic Deep Water. *Paleoceanography* **11**, 157-170.

BIOGRAPHICAL SKETCH

Derrick Richard Newkirk was born in Indianapolis, Indiana. He is the eldest son of Patricia and Richard Newkirk, and the older brother of Ryan Newkirk. His primary education, elementary through high-school, was completed in Greenwood, Indiana. While attending Indiana University ~ Purdue University at Indianapolis he became interested in geology after taking an introductory course taught by Bob Barr. After completion of his four years of eligibility for collegiate soccer, he turned his focus to geology. During his undergraduate education he worked as a lab assistant for Dr. Gabriel Filippelli, and helped Dr. Filippeli's Ph.D. student at the time, Dr. Jennifer Latimer. While working under Dr. Gabriel Filippelli and Dr. Jennifer Latimer he worked on his own research project looking at human impacts on the watershed of Laguna Zoncho, Costa Rica using phosphorus geochemistry. This invaluable experience doing scientific research led him to graduate school. He completed his degree in the summer of 2004 with a Bachelor of Science with a focus in geology. At the University of Florida his research focused on the Miocene carbonate crash using Nd in fossil fish teeth to reconstruct ocean circulation. After completion of the Master of Science degree, he plans on continuing at the University of Florida and pursuing his Ph.D. under the guidance of Dr. Ellen Martin.